CONTROL OF PERMANENT MAGNET SYNCHRONOUS MOTORS THROUGH FOUR SWITCH INVERTER

A DISSERTATION

Submitted in partial fulfilment of the requirement for the Award of the Degree of

MASTER OF TECHNOLOGY
in
Electrical Engineering

by

MANJIT SINGH
Roll No. 31504321
(With specialization in Power Electronics & drives)

Under the Guidance of

Shri Krishan Kumar Sharma
Associate Professor

DEPARTMENT OF ELECTRICAL ENGINEERING
NATIONAL INSTITUTE OF TECHNOLOGY-KURUKSHETRA
KURUKSHETRA-136119 (INDIA)
JUNE 2017

DEPARTMENT OF ELECTRICAL ENGINEERING
NATIONAL INSTITUTE OF TECHNOLOGY
KURUKSHETRA
KURUKSHETRA-136119
HARYANA

CANDIDATES DECLARATION

I hereby declare that the work which is being presented in this dissertation entitled "**CONTROL OF PERMANENT MAGNET SYNCHRONOUS MOTORS THROUGH FOUR SWITCH INVERTER**" towards partial fulfilment of the requirements for the award of the Degree of **Master of Technology** in **Electrical Engineering**, with specialization in **Power Electronics & drives**, is an authentic record of my own work under the supervision of **Shri Krishan Kumar Sharma**, Associate Professor.

The work presented in this dissertation has not been submitted by me for the award of any other degree of this or any other institute. I have taken care in all respects to honour the intellectual property right and have acknowledged the contribution(s) of others for using them for this academic purpose. I will be liable for full or partial violation of copyright or intellectual property right if fount at any stage, even after award of my degree, not my supervisor(s)/ Head of the Department/ Institute.

Date:
Place: Kurukshetra

(MANJIT SINGH)
Roll No. 31504321

CERTIFICATE

This is to certify that ***MANJIT SINGH*** completed his M.Tech. Dissertation under my supervision and the above statement made by my student is correct to the best of my knowledge.

Date:
Place: Kurukshetra

(Shri Krishan Kumar Sharma)
Associate Professor,
Department of Electrical Engineering,
National Institute of Technology Kurukshetra.

ACKNOWLEDGEMENT

At the very outset, I would like to record my heartfelt gratitude to my respectable supervisor Shri Krishan Kumar Sharma, Associate Professor, Department of Electrical Engineering, National Institute of Technology, Kurukshetra. I am grateful for his valuable guidance, constant encouragement and immense help given at various stages of this work. His incisive comments, fruitful discussions and valuable suggestions always edified me to carry out my work.

I also take the opportunity to sincerely thank respectable Dr. Ratna Dahiya, Head of the Electrical Engineering Department, for extending the department facilities to conduct this work.

I also thank the other department employees and my colleagues who directly or indirectly helped in this work.

Last but not the least, I express gratitude to my family for constant motivation during this work.

Date:
Place: Kurukshetra

(MANJIT SINGH)
Roll No. 31504321
M.Tech (Power Electronics & Drives)
National Institute of Technology
Kurukshetra

ABSTRACT

The Suitability of four-switch three-phase (FSTP) inverters as compared to the traditional six-switch three-phase (SSTP) inverters to control the permanent magnet synchronous motor (PMSM) drives has been studied through wide literature. The results of this study are presented in this work. The work is expanded by selecting a latest FSTP inverter which gives nearly sinusoidal ac output voltages of the high amplitude as compared to the earlier texts. A high performance, cost effective, FSTP inverter as a replacement for the traditional SSTP inverter, selected from literature is investigated to control a PMSM motor drive. With no need of output filter this FSTP inverter technique provides pure three-phase sinusoidal output voltage which can be used as the input to the PMSM. The control approach reduces the cost, the switching losses, and the size of the inverter.

A recent single-ended primary-inductance converter (SEPIC) - based FSTP inverter has been investigated and selected for control of the PMSM motor drive in MATLAB – SIMULINK environment.

TABLE OF CONTENTS

CHAPTER-4 FSTP INVERTER FED PMSM DRIVE

CHAPTER-5 CONCLUSION

REFERENCES

LIST OF FIGURES

LIST OF TABLE

CHAPTER-1

INTRODUCTION

Over the last two decades, the permanent magnet synchronous motor (PMSM) has been paid much attention for variable speed drive (VSD) systems due to its high torque to current ratio, large power to weight ratio, high efficiency, high power factor and robustness. PMSM motors are typically used for high-performance and high efficiency motor drives. High-performance is characterized by smooth rotation over the entire speed range of the motor, full control up to zero speed, and fast acceleration and deceleration. To achieve such control, sophisticated control techniques are used. Traditionally six-switch three-phase inverter (SSTPI) is used for this purpose. These inverters have some drawbacks, which involve the losses of the six switches as well as the complexity of the control algorithms and interface circuits to generate six pulse width modulation (PWM) logic signals. In 1984 [1] a new topology consisting only four switches in the three phase inverter is introduced. This four-switch three-phase inverter (FSTPI) has emerged as a competitive topology to the SSTPI resulting into the reduced cost, complexity, size, and switching losses. The FSTPI has these advantages due to the reduced number of power switches and therefore, less number of power conditioning and interfacing circuits of the power switches. Due to the less number of components, the space requirement for the FSTPI is significantly reduced as compared to the SSTPI. This is also facilitated by the reduction in the switching losses and the cooling requirement of the inverter. Traditional FSTPI usually operated at half the dc input voltage; hence, the output line voltage cannot exceed this value. In a recent FSTPI topology [2], the increased amplitude of the output voltage along with its increased closeness with the sinusoidal waveform has shown the significant improvement in the utilization of the dc battery voltage.

Most of the reported works on FSTPI for machine drives did not consider the closed loop vector control scheme, which is essential for high performance drives. Usually, high performance motor drives used in robotics, rolling mills, machine tools, etc. require fast and accurate response, quick recovery of speed from any disturbances and insensitivity to parameter variations. The dynamic behavior of an ac motor can be significantly improved using vector control theory where motor variables are transformed

into an orthogonal set of d-q axes such that speed and torque can be controlled separately. Fig. 1.1 shows classification of various kinds of motors.

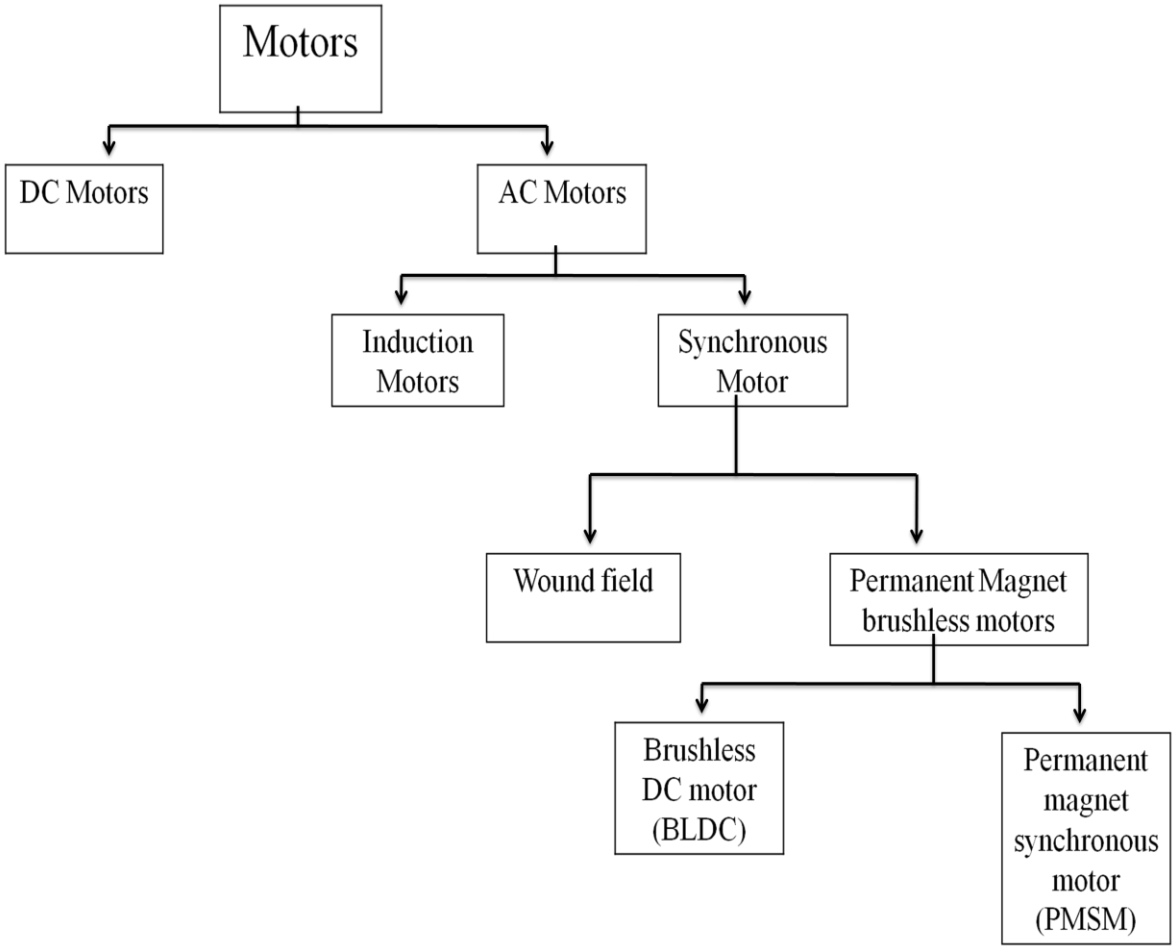

Fig. 1.1 Classifications of motor.

Most of the past research on variable speed PMSM motor drives mainly concentrated on the development of the efficient control algorithms for high performance drives. However, the cost, simplicity and flexibility of the overall drive system which become some of the most important factors did not get that much attention to the researchers. That is why, despite tremendous research in this area most of the developed control system failed to attract the industry.

CHAPTER-2

Permanent Magnet Synchronous Motors

2.1 Permanent Magnet Brushless Motors

Permanent magnet brushless (PMBL) motors are broadly classified as PMSM motors and BLDC motors. There principle of operation and comparison are as follows.

2.1.1 Principle of Operation of PMSM

A PMSM motor is a synchronous motor that uses permanent magnets rather than windings in the rotor as shown in Fig. 2.1. Electronic excitation control with integrated power inverter and rectifier, sensor, and inverter electronics is required for practical operation.

The PMSM motor is an AC synchronous motor whose field excitation is provided by permanent magnets, and has a sinusoidal Back EMF waveform.

- With permanent magnets the PMSM motor can generate torque at zero speed
- higher torque density versus AC Induction Motors (ACIM), i.e., smaller frame size for same power
- high efficiency operation
- requires digitally controlled inverter for operations

PMSM motors are typically used for high-performance and high-efficiency motor drives. High-performance motor control is characterized by smooth rotation over the entire speed range of the motor, full torque control at zero speed, and fast acceleration and deceleration. To achieve such control, vector control techniques are used for PMSM motors. The vector control techniques are usually also referred to as field-oriented control (FOC). The basic idea of the vector control algorithm is to decompose a stator current into a magnetic field-generating part and a torque generating part. Both components can be controlled separately after decomposition. Then, the structure of the motor controller (vector control controller) is almost the same as a separately excited DC motor, which simplifies the control of a PMSM motor.

Characterized by permanent magnets on rotor known for

- Its simplicity and low maintenance
- No copper loss on rotor
- High efficiency

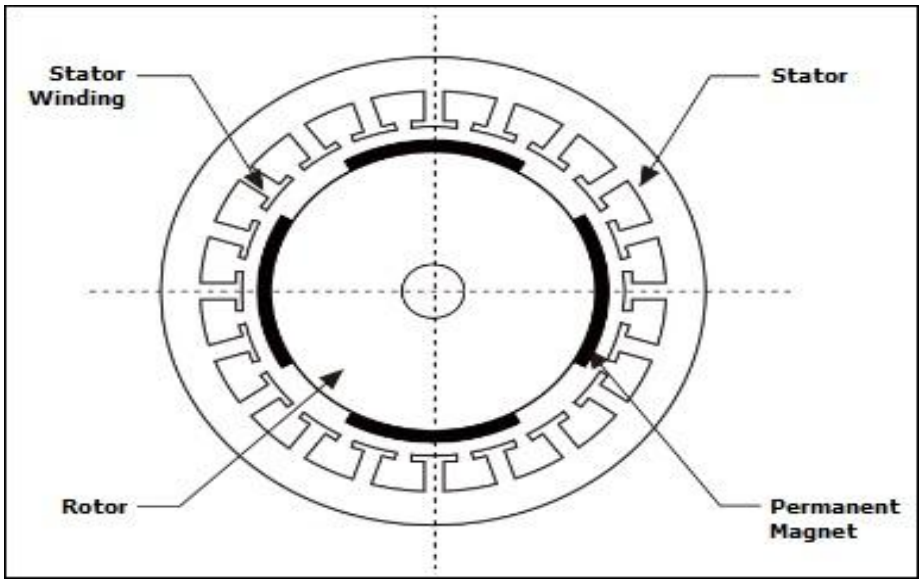

Fig. 2.1 Permanent magnet synchronous motor.

PMSM motor is widely used in appliances, robots, and hybrid Electric vehicle and many other motor applications. PMSM motor has a small size, high efficiency and high performance. Field-Oriented control is efficiently used method to control the torque as well the speed of PMSM motor. This presents a mathematical model of PMSM motor, which is multiple stator winding with constant excitation feeds from the permanent magnet which is mounted on the rotor. Only surface permanent magnet synchronous motor is considers in this. Power switching electronic is used to generate the desired voltage/current from DC source. PWM technique controls the switching power electronic by creating a control signals which are applied to their gates. The whole circuit of the inverter based on space vector PWM. FOC, or vector control, is implemented via Digital Signal Processors to control PMSM motor. Clarke and Park transformations are applied to '*abc*' coordinate frame of permanent magnet synchronous motor model to get the '*qd*' coordinate frame that is used in field oriented control technique. Hence, the developed

torque and the magnetizing the ux component are controlled separately. Since the rotor angle is required for Park transformation, field oriented control is classified into two types; indirect, or called sensorless, and direct, or called sensorless, method. In this only sensorless FOC is presented. PI controller is used to control the motor speed and torque. PI controllers are design using frequency response method and symmetric optimum method. The whole system is simulated based on the mathematical model of PMSM motor and field-oriented control method with designed PI controllers. Simulation results show the PMSM motor have a perfect dynamic response. Digital signal processors are a high speed processor which can implement the field oriented control algorithms and compute the parameter in real time. A Texas Instruments kits and software are used to implement field-oriented control of permanent magnet synchronous motor. The paper includes a short review of DSP controller. Implementation of field-oriented control of PMSM motor shows satisfactory performance yielding low torque ripples and low speed ripples.

PMSM motors are applied to various fields such as railway vehicles, road electric vehicles (EVs), road hybrid electric vehicles (HEVs), electrical home and industrial appliances, etc. Because of their compactness, high power density and high efficiency, PMSM motor as traction motor of EVs or HEVs widens high-speed drive region, gives fast torque response is more compact, and more reliable. To widen drive region and to achieve fast torque response of PMSM motor, high DC link voltage is simple solution. Expanding battery module, however, is undesirable solution as cost, weight and installation space. Thus operating PMSM motor in the over modulation range is required. By operating PMSM motor in the over modulation range of inverter, maximum of 27% higher voltage can be obtained from the same DC link voltage compared to the operation in the linear range. Therefore, operation of PMSM motor in the over modulation range has been researched. Position sensorless control is also an important research area of PMSM motor drive. In order to obtain a high torque performance, a vector control is very common method. And information of rotor position is necessary for the current vector control. Sensors to detect the rotor position, however, make some problems which are cost, power/torque density. And the sensors can negatively affect the robustness of the PMSM motor, both electrically and mechanically. Therefore, position sensorless control

is required in some cases. In the over modulation range, however, the inverter output contains low-order harmonic voltage, and it destabilizes both the current control system and position estimation system. Though open loop controllers are one solution to avoid destabilization, however these control system has to change controller for drive in the over modulation range. Authors proposed position sensorless Torque control system with harmonic estimator which is able to operate both in linear and over modulation range by single controller and were evaluated under torque control condition.

In today's fast changing world, PMSM motors – commonly used in industrial automation for traction, robotics or aerospace – require greater power and high level of intelligence. Cutting-edge semiconductor solutions form great promise and deliver high quality and innovative technologies. By using the software tools the complexity and cost of integrating specific features into the system can be reduced. This way the right products, application kits and support are found to optimally control permanent magnet synchronous motors. Additional motor control applications are in the battery powered applications, home and building and industrial automation.

The PMSM motor is intermediary between an induction motor and BLDC motor. Like a BLDC motor, it has a permanent magnet rotor and windings on the stator. However, the stator structure with windings constructed to produce a sinusoidal flux density in the air gap of the machine resembles that of an induction motor. The power density of PMSM motors is higher than that of induction motors with the same ratings in which the stator power contribution to the magnetic field is absent. Today, these motors are designed to be more powerful while also having a lower mass and lower moment of inertia.

2.1.2 Principle of operation of BLDC motor

BLDC motor may be described as electronically commutated motor which does not have brushes. This motor is highly efficient in producing large amount of torque over a vast speed range.

Before explaining working of BLDC motor, it is better to understand function of brushed motor. In brushed motors, the magnetic field is produced either by permanent magnets of stator or by the field winding placed on the stator and fed by the DC supply.

When the DC supply is applied to the armature through mechanical commutator and brushes, an alternating current flows in the armature conductors. Since these current carrying armature conductors are placed in the magnetic field of the field magnets, the forces and hence the torques are applied on the conductors which rotates the armature. The nature of the EMF in the armature conductor is flat-topped (near to trapezoidal).

BLDC motor works on the principle similar to that of a conventional DC motor, i.e., the Lorentz force law which states that whenever a current carrying conductor placed in a magnetic field it experiences a force. As a consequence of reaction force, the magnet will experience an equal and opposite force. In case BLDC motor, the current carrying conductor is stationary while the permanent magnet moves.

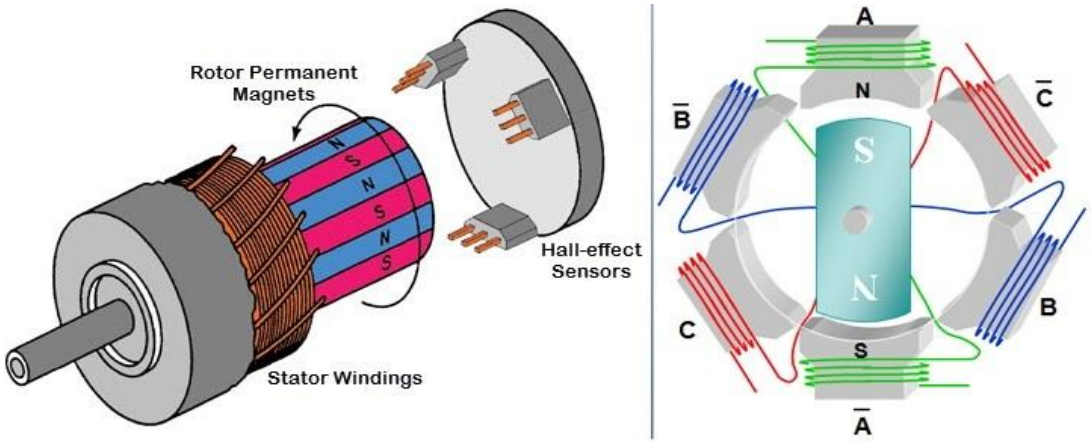

Fig. 2.2 Brushless DC motor.

As shown in Fig. 2.2, when the stator coils are electrically switched by a supply source, it becomes electromagnet and starts producing the uniform field in the air gap. Though the source of supply is DC, switching makes to generate an AC current waveform with rectangular shape. Due to the force of interaction between electromagnet on stator and permanent magnet rotor, the torque is applied on the rotor to keep it rotating.

Motor stator is excited based on different switching states. With the switching of windings as High and Low signals, corresponding winding energized as North and South poles. The permanent magnet rotor with North and South poles align with stator poles causing motor to rotate.

Observe that motor produces torque because of the development of attraction forces (when North-South or South-North alignment) and repulsion forces (when North-North or South-South alignment). By this way motor moves in a clockwise direction.

Based on this signal from sensor, the controller decides particular coils to energize. Hall-effect sensors generate Low and High level signals whenever rotor poles pass near to it. These signals determine the position of the shaft.

2.1.3 Comparison of PMSM and BLDC Motors

A BLDC motor and PMSM motor consist of a permanent magnets, which rotates (the rotor), surrounded by three equally spaced windings, which are fixed (the stator). Current flows in each winding producing a magnetic field vector, which sums with the fields from the other windings. By controlling currents in the three windings, a magnetic field of arbitrary direction and magnitude can be produced by the stator. Torque is then produced by the attraction or repulsion between this net stator field and the magnetic field of the rotor.

The BLDC and PMSM motors can be the same or different depending on the researcher's views. Basically they are synchronous motors with permanent magnets attached on their rotors. Some researchers define a BLDC motor is a PMSM motor with trapezoidal BEMF, while a BLAC motor is a PMSM motor with sinusoidal BEMF. The drive techniques for BLDC motors and PMSM motors are quite different. In BLDC machine, the stator winding is concentrated. Hence the stator EMF waveform will be trapezoidal, whereas in PMSM motor the stator winding is distributed. Hence the stator EMF waveform is sinusoidal. As far as rotor is concerned both have permanent magnets.

The main difference in the rotor shape, nature of armature winding and nature of armature current are as follows.

- In BLDC motor the magnet shape and the concentric armature winding provide trapezoidal EMF in the armature winding while the rectangular armature currents are forced through electronic commutation.

- In PMSM motor the magnet shape and the distributed armature winding provide sinusoidal EMF in the armature winding while the sinusoidal armature currents are forced through electronic commutation.

2.2 Control of PMSM motors

PMSM motors are typically used for high-performance and high-efficiency motor drives. High-performance motor control is characterized by smooth rotation over the entire speed range of the motor, full torque control at zero speed, and fast acceleration and deceleration. To achieve such control, vector control techniques are used for PMSM motor. The vector control techniques are usually also referred to as FOC. The basic idea of the vector control algorithm is to decompose a stator current into a magnetic field-generating part and a torque generating part. Both components can be controlled separately after decomposition. Then, the structure of the motor controller (vector control controller) is almost the same as a separately excited DC motor, which simplifies the control of a PMSM motor [3].

In PMSM motor speed control system, some constraints are paid close attention because of their affects on system performance, for example, the restrictions on the amplitude of voltage, current or torque. Two commonly used methods to handle the constraints are Anti-Windup and MPC. Wherein, Anti-Windup method has some advantages such as a simple structure, offline design and very small amount of calculation. However, MPC is more potential for the systems containing multivariable constraints and can obtain the optimal control law with solving optimization problems online [4].

The approximate linearization model of PMSM motor speed control system is used to design a linear MPC speed controller to meet the constraints on the speed and the current. Shows the feedback linearization method is combined with MPC to achieve the speed control and meet current constraints. Proposed the piecewise feedback Anti-Windup method to design PID speed controllers and the overshoot of speed is effectively suppressed over a large dynamic range.

This presented a simple and accurate linearization method for PMSM motor speed control system, on this basis, a linear MPC controller to ensure the closed-loop stability of systems is designed by defining the terminal constraint set conditions. Finally, the performance comparison of MPC and Anti-Windup is fulfilled through simulation.

2.2.1 Field-Oriented Control (FOC)

FOC of PMSM motor is one important variation of vector control methods as given in Fig. 2.3. The aim of the FOC method is to control the magnetic field and torque by controlling the d and q components of the stator currents or relatively fluxes. With the information of the stator currents and the rotor angle a FOC technique can control the motor torque and the flux in a very effective way. The main advantages of this technique are the fast response and the little torque ripple. The implementation of this technique will be carried out using two current regulators, one for the direct-axis component and another for the quadrature axis component, and one speed regulator**.**

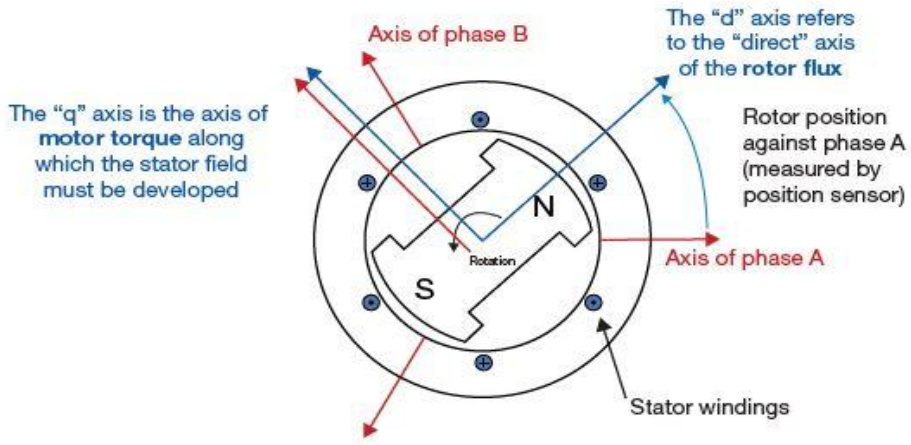

Fig. 2.3 Field-oriented control vector explanation

PMSM machine is the BLDC motor designed for low voltage electronic equipment. In their initial stage the operations of PMSM motor were limited to simple DC motor circuits with low power input and high performance index. However, with later improvement in machines introduced the applications of PMSM motor in heavy industrial equipment considering the benefits over conventional motors. The panorama of

PMSM motor has covered areas of automobiles, military, precision tools, Medical instruments etc. However PMSM motors perform poorly with open-loop scalar V/Hz control, since there is no rotor coil to provide mechanical damping in transient conditions.

PMSM motors are widely used in appliances, robots, and hybrid Electric vehicle and many other motor applications. PMSM Motor has a small size, high efficiency and high performance. FOC is an efficiently used method to control the torque as well the speed of permanent magnet Synchronous motor. This presents a mathematical model of permanent magnet synchronous motor, which is multiple stator winding with constant excitation feeds from the permanent magnet which is mounted on the rotor. Only surface PMSM motor is considers in this. Power switching electronic is used to generate the desired voltage/current from DC source. PWM technique controls the switching power electronic by creating a control signals which are applied to their gates. The whole circuit of the inverter based on SVPWM. FOC, or vector control, is implemented via Digital Signal Processors to control permanent magnet synchronous motor. Clarke and Park transformations are applied to '*abc*' coordinate frame of PMSM motor model to get the '*qd*' coordinate frame that is used in field oriented control technique. Hence, the developed torque and the magnetizing the u_x component are controlled separately. Since the rotor angle is required for Park transformation, field oriented control is classified into two types; indirect, or called sensorless, and direct, or called sensorless, method. In this only sensorless FOC is presented [3]. PI controller is used to control the motor speed and torque. PI controllers are design using frequency response method and symmetric optimum method. The whole system is simulated based on the mathematical model of PMSM motor and field-oriented control method with designed PI controllers. Implementation of field-oriented control of PMSM motor shows that motor has satisfactory response in terms of torque ripple and speed response.

FOC is the most popular control technique used with PMSM motor. FOC technique operates smoothly and provides maximum torque, full speed range and instantaneous acceleration and deceleration by controlling the *iq* and *dq* currents for three phase voltage supply in lower performance applications. To convert the low voltage input in high voltage for motor coordination, the FOC is implemented with a voltage inverter.

The capability of inverter to modulate the voltage signifies the operating range of PMSM motor. The difference in the input voltage pulse and the required modulation voltage are subject of PID controllers installed in FOC controllers [5]. However, to generate maximum torque at zero speed and maximize the overall performance of PMSM motor the inverters are generally operated in over modulation range. The difference in actual flux and torque compared with estimated values are basis for switching of inverters. The gate (electric) pulses for control of inverter are derived from a standard unit known as Space Vector Pulse Width Modulation.

As we mentioned before, the goal of FOC is to control the developed torque and the magnetizing field, individually, by analyzing, transforming, and making PMSM motor behaves like a separate excited DC machine. In general, DC machines have the armature winding in the rotor while the field winding in the stator. Now the DC machine torque control, one can recall the orientation of the armature MMF. The commutator keeps the angle between the MMF and field flux 90 degree. In another ward, the action of commutator is to reserve the direction of the armature winding currents as the coils pass the brush position such that the armature current distribution is fixed in space no matter what the rotor speed is Fig. 2.3 shows a diagram of a DC machine with the MMF and Field axis. The field flux λ_f , and armature MMF are orthogonal, therefore, the flux is unaffected by the armature current, as given in Eqn. 2.2 Ia.

There are two basic results:

1- The induced voltage E_a is proportional to the rotor speed ω_m:

$$E_a = \frac{p}{2} \lambda_{af} \omega_m \qquad (2.1)$$

2- The electromagnetic torque is proportional to the armature current:

$$T_e = \frac{p}{2} \lambda_{af} I_a \qquad (2.2)$$

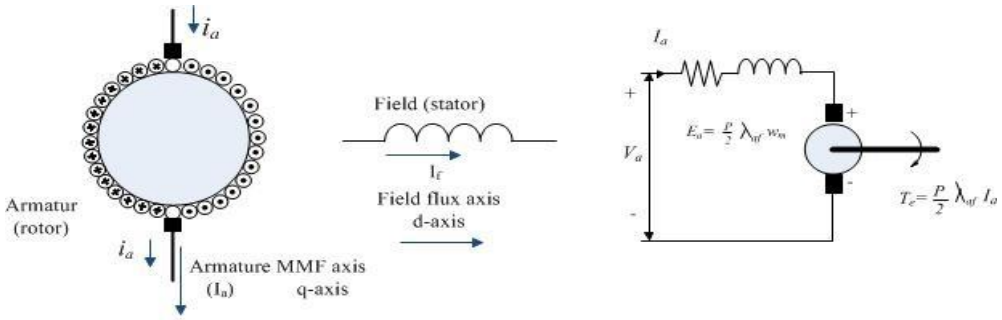

Fig. 2.4 DC Motor Diagram.

Where λ_{af} is the flux produced by field current which links the armature winding Eqn. 2.3.

$$\lambda_{af} = \frac{L_{af}}{L_{If} + L_{af}} \lambda_f \tag{2.3}$$

$$= \frac{L_{af}}{L_f} \lambda_f \tag{2.4}$$

L_{af} is mutual inductance between field and armature winding. L_f is field leakage inductance and L_f is the field self inductance.

Therefore

$$T_e = \frac{p}{2} \frac{L_{af}}{L_f} \lambda_f I_a \tag{2.5}$$

Therefore, the requirements for torque control in DC machine are:

1- An independent controlled I_a to overcome the effects of armature resistance, leakage inductance and induced voltage.

2- An independent controlled or constant value of field flux.

3- A separately controlled orthogonal spatial angle between flux and MMF to avoid the interaction of MMF and field flux.

Fig. 2.5 shows a schematic diagram of FOC. It starts by computing the three phase current of the PMSM motor by measuring i_a and i_b only, since $i_a+i_b+i_c = 0$. Thus two sensors are only needed. The sensor is usually a shunt resistance. By using Clarke transformation, i_α and I_β are found. Rotational Park transformation converts the current from "$\alpha\beta$" to "dq" coordinate frame. I_{dref} and I_{qref} are the current reference signals to generate error signals with id and iq. These error signals are fed into the Proportional-Integral (PI) controller to regulate and send as vd and vq. Inverse rotational Park transformation is converted vd and vq to v_α and v_β which are fed to SVPWM [6]. SVPWM generated signals apply to VSI to create the required output voltage. Moreover, the rotor angle is encoded, which is used in dq transformation and calculates the instantaneous rotor speed ω_m. Ω_m is compared to ω_{mref} , which is the reference speed, to obtain speed error signal. This error is fed to PI controller whose output is ω_{qref}.

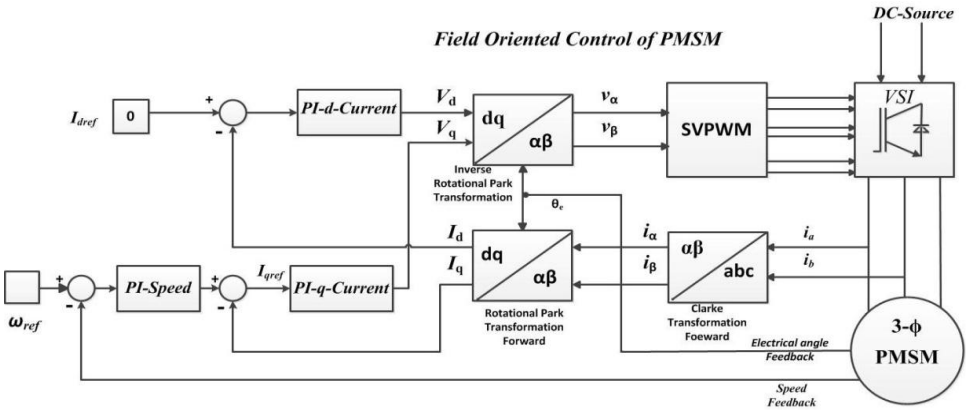

Fig. 2.5 Basic diagram of FOC of PMSM motor.

2.2.2 Direct Torque Control (DTC)

Direct Torque Control is one of the high performance control strategies designed for AC machines in 1980s. the DTC is implemented by selecting proper voltage space vector (VSV) according to the switching status of the inverter which depends upon the error values between the reference flux linkage and torque with their measured real values obtained from calculations in stationary reference frame by means of simply detecting the motor voltage and currents. The DTC scheme has already been realized successfully in induction motor drives and nowadays for PMSM motor also. Therefore

there are lots of questions and techniques needed to and deserved to be investigated further in this aspect. Aiming at the DTC of PMSM motor drives this paper illustrates the theoretical basics of DTC in PMSM motor drives firstly and then explains the application of DTC to PMSM motor for the purpose of utilizing the successful and matured technique of DTC to solve the problems in implementation of DTC in PMSM motor [7].

DTC method has been first proposed for induction machines. This concept can also be applied to synchronous drives. The DTC technique is different from the conventional vector control method, where torque is controlled in the rotor reference frame via current control loops. But the conventional DTC strategy has serious ripples of the electromagnetic torque and flux linkage inevitably, so its steady state performance is poor, and the inverter has variable switching frequency. Many researchers have devoted to the improvement of the steady state performance of the basic DTC, especially for induction machine since the first industrial product has been produced in 1996. In the late 1990s, DTC method has been proposed for permanent magnet synchronous motor, as well as the advantages for induction motor. However, new problems appear regarding application of zero vectors. This is especially true at a low speed, when the zero voltage vectors application on the PMSM motor holds the torque rather than decreases it. As well as improving dynamics, deletion of zero vectors also causes more significant torque and flux ripples in steady state, and complicates the control of the motor smoothly in the low speed range. Therefore, the way of minimizing torque ripples becomes the main research subject in a DTC of PMSM motor [8].

Space vector modulation DTC is a technique to reduce the ripples of the electromagnetic torque and flux linkage. Space vector modulation techniques have several advantages that are offering better DC bus utilization, lower torque ripples, lower total harmonic distortion in the AC motor current, lower switching loss, and easier to implement in the digital systems.

In general, there are two control methods used for the PMSM motor; field oriented control and direct torque control [9, 10]. The AC drives in which flux oriented control (FOC) is used field control leads to flux control. Here, rotor flux space vector is calculated and controlled by using the angular velocity which is derived from the speed

feedback and the stator current vector. The greatest drawback of the flux vector control is the need for a tachogenerator or an encoder for high accuracy. This need definitely increases the costs of the system. The basic principle of DTC is to directly select the stator voltage vectors according to the errors between the reference and actual values of the torque and stator flux. Torque and flux are resolved and directly controlled using nonlinear transformations on hysteresis controllers, without performing coordinate transformations. A double layer hysteresis band controller is utilized for stator flux control and a three-layer hysteresis band controller is used for torque control. DTC is an alternative to field oriented control method in high performance applications due to the advantages of reduced computations, since the torque and flux estimators in DTC requires and relies on the parameters identification and accuracy of the estimations, the estimation of the electromagnetic torque is essential for the entire system performance. In classical PWM and flux vector controlled drives, voltage and frequency are used as basic control variables and that are modulated and then applied to the motor [11]. This modulator layer needs an additional signal processing time and restricts the torque and speed response. The key notion behind DTC is to directly steer the stator flux vector by applying the appropriate voltage vector to the stator windings. This is done by using a pre-designed switching table to directly update the inverter's discrete switch positions whenever the variables to be controlled, the electromagnetic torque and the stator flux, exceed the hysteresis bounds around their references. The switching table is derived on the basis of the desired performance specifications on the controlled variables also include the balancing of the inverter's neutral point potential around zero.

2.2.2.1 Determination of the voltage space vector

The main principle of DTC is determination of correct voltage vectors using the appropriate switching table. The determination process is based on the torque and stator magnetic flux hysteresis control. Stator magnetic flux can be calculated using Eqn. 2.6.

$$\bar{\psi}_s = \int_{t}^{t+\Delta t} \left(\bar{u}_s - R_s \bar{i}_s \right) dt \qquad (2.6)$$

Eqn. 2.6 shows that the stator magnetic flux and the voltage space vector are in the same direction. Therefore, amplitude and direction control of the stator magnetic flux is possible by selecting the suitable voltage space vectors. Voltage vector plane is divided into six parts as shown in Fig. 2.6. Two adjacent vectors that yield the lowest switching frequency are selected in order to increase or decrease the amplitude respectively [12].

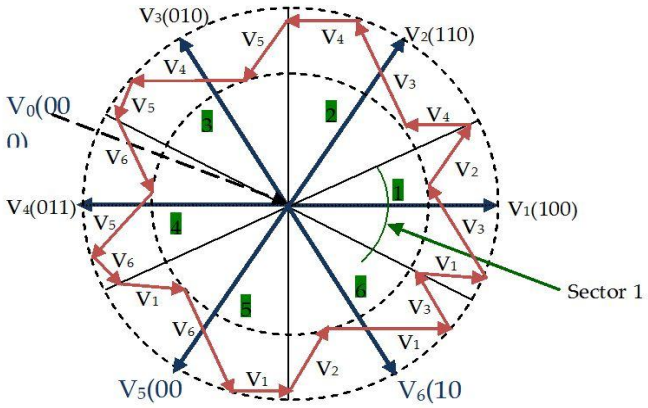

Fig. 2.6 Vectors of space vector modulation.

Here, when the stator magnetic flux is moved clockwise in sector 1, voltage space vector v_2 is selected in order to increase the stator magnetic flux amplitude and voltage space vector v_3 is selected in order to decrease the amplitude. When the stator magnetic flux moves clockwise, if still in section 1, v_6 is used to increase the amplitude and v_5 is used to decrease the amplitude. The torque of the PMSM motor can be controlled using DTC by means of controlling the stator magnetic flux rotation speed in cases where the stator magnetic flux amplitude is kept constant. Since the magnets on the rotor are continuously rotating, stator magnetic flux does not change when v_0 and v_7 zero vectors are used. Zero vectors can be used to estimate the initial position of the rotor by a fixed active voltage vector while limiting current by applying zero vectors. In this position data is not used; therefore, zero vectors are not used within DTC for PMSM motor [12, 13]. Table 1 shows the suggested switching sequences. For these different states, the hysteresis controllers can be used as flux and torque hysteresis controllers.

Ψ	T	θ					
		θ(1)	**θ(2)**	**θ(3)**	**θ(4)**	**θ(5)**	**θ(6)**
1	**1**	V_2 (110)	V_3 (100)	V_4 (101)	V_5 (001)	V_6 (011)	V_1 (010)
	0	V_7 (111)	V_0 (000)	V_7 (111)	V_0 (000)	V_7 (111)	V_0 (000)
	-1	V_6 (101)	V_1 (001)	V_2 (011)	V_3 (010)	V_4 (110)	V_5 (100)
0	**1**	V_3 (010)	V_4 (110)	V_5 (100)	V_6 (101)	V_1 (001)	V_2 (011)
	0	V_0 (000)	V_7 (111)	V_0 (000)	V_7 (111)	V_0 (000)	V_7 (111)
	-1	V_5 (001)	V_6 (011)	V_1 (010)	V_2 (110)	V_3 (100)	V_4 (101)

Table 2.1 switching vector.

In Table 2.1(a). ψ denotes stator magnetic flux hysteresis controller output, T denotes torque hysteresis controller output, and θ represents magnetic flux sector. These vectors are selected in order to provide the stator flux error within 2Δψs bandwidth and the actual torque error in the $2t\Delta_e$ bandwidth at each switching period. The flux hysteresis controller output is dψs. If an increase is needed for flux, it is assumed that d 1 ψs = and when a decrease is needed, it is assumed that d 0 ψs = 0. Two level hysteresis controllers are determined by Eqn. 2.7.

$$d\psi_s = \begin{cases} 1, & |\psi_s| \leq \psi_{sref} - \Delta\psi_s \\ 0, & |\psi_s| \geq \psi_{sref} + \Delta\psi_s \end{cases} \tag{2.7}$$

In direct torque method, three level torque comparator is used to select whether the inverter output voltage vector should be a torque-increasing vector or a torque-reducing vector. The appropriate vector is then applied for the duration of the sampling period. At low speed the torque increasing vectors are very effective at increasing the torque, whereas the torque reducing vectors are less effective. In contrast, at high rotor speeds, the torque-increasing vectors are less effective, whereas the torque reducing vectors are more effective. The result of this is that, at low speed, the torque tends to make a considerable excursion above the maximum torque hysteresis limit.

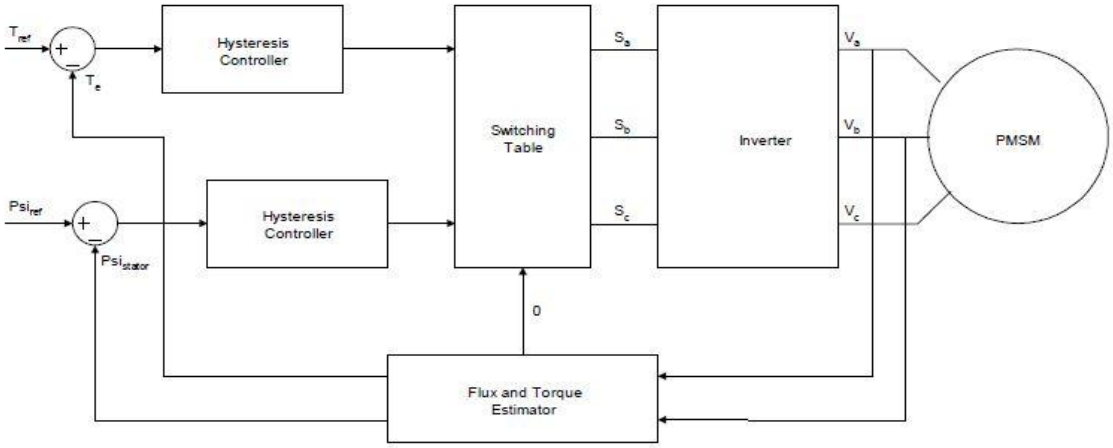

Fig. 2.7 Schematic diagram of DTC for PMSM motor.

2.2.3 Model predictive control (MPC)

A Model Predictive Control (MPC) algorithm applied to electrical drives. The main contribution is a comprehensive and detailed description of the controller design process that points out the most critical aspects and gives also some practical hints for implementation. As an example, the MPC is developed for a permanent magnet synchronous motor drive. Speed and current controllers are combined together, including

all of the state variables of the system, instead of keeping the conventional cascade structure. This way the controller enforces both the current and the voltage limits.

Its strategies are based on an explicit and identifiable model of the controlled system [14], which is used to pre-calculate the behavior of the plant and to choose an optimal value of the control variables. Because of the computational effort required by MPC, its implementation has been formerly restricted to slowly varying systems, as chemical processes, in which the time step of the discretization is long enough to allow the complete execution of the control algorithm. As the performance of the available computing hardware has rapidly increased and new faster algorithms have been developed, it is now possible to implement MPC for fast systems with shorter time steps.

Electrical drives are of particular interest for the application of MPC for at least two reasons:

1) Their quite accurate linear models can be obtained by both analytical means and identification techniques;

2) Bounds on drive variables play a key role in the dynamics of the system. Actually, two main approaches are available to deal with systems constraints: the conventional anti–windup techniques, with their manifold variants, widely used in the PI controllers, and MPC [15]. It is worth to note that the difficulty in establishing constraints on the states have also limited the application of conventional state space controllers.

In spite of the mentioned advantages, MPC applications to electrical drives are still largely unexplored and they involve only few research laboratories. For example, generalized predictive control (GPC) – a special case of MPC – has been applied to induction motors first for the current regulation only and, later, for the speed and current control. In the more general MPC solution has been adopted for the design of the current controller in the same drive. In other works MPC has been used as a current or a torque/flux controller, directly driving the inverter states. The main contribution of this paper is a comprehensive and detailed description of the design process of an MPC controller for an electrical drive, pointing out the most critical aspects and giving some practical hints for the design and the implementation, and some suggestions for future studies and developments. As an example of application, the MPC is applied to the

control of a PMSM motor. Speed and current controllers are combined together in a single MPC that includes all the state variables of the system, instead of keeping the conventional cascade structure. In this way it is possible to enforce all the constraints of the system namely current and voltage limits in the controller. Opposite to previous works, this also considers the motional coupling effect between the direct and quadrature axes of the motor. This approach exploits the main advantages of MPC, i.e. its capability of systematically coping with hard constraints on inputs and states, and its suitability for directly addressing multi-variable systems. These are the null steady-state error in the presence of unknown load and parameters mismatch of the model and the preservation of stability when a low-pass filter is introduced in the feedback path, especially in the speed measurement.

In PMSM motor speed control system, some constraints are paid close attention because of their affects on system performance, for example, the restrictions on the amplitude of voltage, current or torque. Two commonly used methods to handle the constraints are Anti-Windup and MPC. Wherein, Anti-Windup method has some advantages such as a simple structure, offline design and very small amount of calculation. However, MPC is more potential for the systems containing multivariable constraints and can obtain the optimal control law with solving optimization problems online.

The approximate linearization model of PMSM motor speed control system is used to design a linear MPC speed controller to meet the constraints on the speed and the current. Shows the feedback linearization method is combined with MPC to achieve the speed control and meet current constraints. Proposed the piecewise feedback Anti-Windup method to design PID speed controllers and the overshoot of speed is effectively suppressed over a large dynamic range. This presented a simple and accurate linearization method for PMSM motor speed control system, on this basis, a linear MPC controller to ensure the closed-loop stability of systems is designed by defining the terminal constraint set conditions.

Advantages of PMSM motor drives over other drives are higher power factor operation, higher torque to inertia ratio and higher efficiency. In recent years, new control strategies have been studied for the current control of power inverters. Among them,

MPC has been applied for the control of power converters due to its several advantages, like fast dynamic response, easy inclusion of nonlinearities and constraints of the system, and the flexibility to include other system requirements in the controller. A cost function represents the desired behavior of the system. MPC is an optimization problem where a sequence of future actuations is obtained by minimizing the cost function. The first element of the sequence is applied, and all the calculation is repeated every sample period. Due to the fast sampling times used in the control of power converters, solving the optimization problem of MPC online is not practical. One approach is to use an explicit solution of MPC, solving the optimization problem offline. The resulting controller is a search tree or a lookup table and can be implemented without big computational effort. This solution has been used for the control of a DC–DC converter and a drive system. Considering that power converters are systems with a finite number of states, given by the possible combinations of the state of the switching devices, the MPC optimization problem can be simplified and reduced to the prediction of the behavior of the system for each possible state. Then, each prediction is evaluated using the cost function, and the state that minimizes it is selected. This is also a different approach that has been successfully applied for the current control in a three-phase inverter and a matrix converter power control in an active front-end rectifier and torque and flux control of an induction machine [16].

MPC uses an explicit model of system to predict future trajectory of system states and outputs. The optimization yields an optimal control sequence as input and only the first input from the sequence is used as the input to the system. At the next sampling interval, the horizon is shifted and the whole optimization procedure is repeated. The main reason for using this procedure, which is called receding horizon control (RHC), [17, 18, 19] is that it allows compensating for future disturbance and modeling error. The basic structure of model predictive control is depicted in Fig. An explicit model of the system is used to predict output response of the future chain $\hat{y}$. Based on the predicted system output and current system output, the error is calculated. The errors, then, are fed to the optimizer. In the optimizer, the future optimal control sequence Δu, is calculated based on the objective function and system constraints. The state space model of the

system is used in the model predictive control. The general discrete form of the state space model used in model predictive control is of the form:

$$x(k + 1) = A_x(k) + B_u(k) + E_d(k) + F_w(k) \tag{2.8}$$

$$y(k) = C_x(k) \tag{2.9}$$

Where k is the sampling instant, x is the state vector, u is the input vector, d represents system disturbance and w represents system noise model. A, B, C, E and F are coefficients of system state space model and reflect the PMSM motor model. The final aim of MPC is to provide zero output error with minimal control effort. Therefore, the cost function J that reflects the control objectives is as follows:

$$J(n) = \sum_{k=1}^{N_p} \mu_k (y'(N+K) - y_{ref}(n+k))^2 \tag{2.10}$$

$$+ \sum_{k=1}^{Nc} v_k \Box u(n+k)^2 \tag{2.11}$$

Where μ_k and v_k , respectively, are the weighting factors for the prediction error and control energy, y(n + k) is the k^{th} step output prediction, y_{ref}(n + k) is the k^{th} step reference trajectory and u(n + k) is the k^{th} step control action. Where the first term reflects the future output error and second term reflects the consideration given to the control effort. The predicted output vector has dimension of 1 × N_p where N_p is the prediction horizon. u is control action vector with dimension of 1×N_c that N_c is control horizon. In the MPC, the control horizon, N_c, is always smaller than or equal to prediction horizon (N_p). μ_k and v_k are reflecting the weights on the predicted error of predicted outputs and change in the control action.

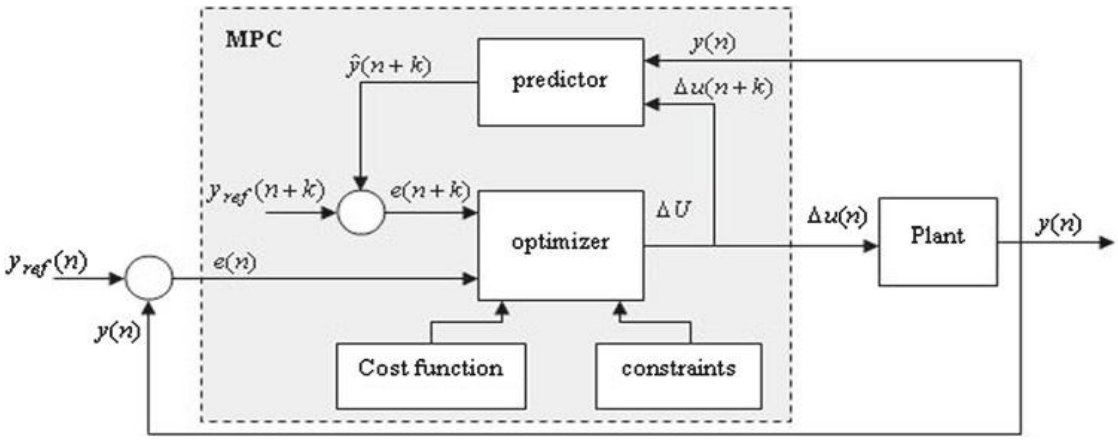

Fig. 2.8 Basic structure of model predictive control (MPC)

$$\begin{aligned} u_{min} \le u(n+k) \le u_{max}\,, \quad \Delta u_{min} \le \Delta u(n+k) \le \Delta u_{max} \\ x_{min} \le x(n+k) \le x_{max}\,, \quad \Delta x_{min} \le \Delta x(n+k) \le \Delta x_{max} \\ y_{min} \le y(n+k) \le y_{max}\,, \quad \Delta y_{min} \le \Delta y(n+k) \le \Delta y_{max} \end{aligned} \tag{2.12}$$

The constraints of MPC include constraints of magnitude and change of input, state and output variables that can be defined in the following form Eqn. 2.12.

CHAPTER-3

Four Switch Three Phase Inverter

In earlier times, when Four-switch three-phase inverter (FSTPI) were generally used as course of action component minimized and which was first in use with three-phase induction motor in as early as 1984 [1]. It consists of variable speed drives using three-phase inverters and squirrel cage induction machines and has already found many practical applications. Certain applications, however, still require a further cost reduction for the drive. Regarding the drive motor, important reduction in material cost may be obtained by raising the speed, while the reduction of the number of power semiconductor device components in the converter should be the main consideration for reducing the cost of the control subsystem. The use of transistors instead of thyristors eliminates the force commutating components and, when properly designed, presents distinct advantages for drives in the power range up to 50 KVA. A further reduction in components is possible by considering alternatives to the conventional three-phase bridge configuration for a voltage-fed inverter, since this circuit uses six switching devices and six reactive power diodes. These Considerations lead to a bridge circuit with only four switching devices and four reactive power diodes. It has been shown in the past that a two-level current control can be implemented to yield quasi-sinusoidal currents in the three load phases. Fundamentally, however, there are two control possibilities for this type of three-phase Inverter Bridge, i.e., current source operation (two-level current control) and voltage source operation (PWM). Due to the limitations of the current source method, the second option is also used in practice. In one method of pulse width modulation a four switch circuit is suggested in order to obtain PWM phase voltages in all three phases, using only two modulated voltages. As this phase asymmetric PWM (PAPWM) leads to series of positive, negative, and zero sequence voltages, the method is evaluated theoretically against a six switch circuit with PWM, including influences on additional losses and torque pulsations. Furthermore, by operating a machine off a 50-hz supply, an experimental evaluation of residual no ideal effects can be made [20, 21, 22]. Operation of the same machine at the same operating point in the torque speed plane by

feeding from both a six switch and a four switch circuit with PWM, two-level current control, and PAPWM, respectively, also enables an experimental comparison to be made.

Many research works are focusing in the development of the efficient control algorithms for high performance variable speed induction motor (IM) drives. Induction motor has been operated as a work horse in the industry due to its easy build, high robustness and generally satisfactory efficiency. Recent development of high speed power semi conductor devices, three phase inverters take part in the key role for variable speed AC motor drives. Traditionally, SSTPIs have been commonly utilized for variable speed IM drives; this involves the losses of the six switches as well as the complexity of the control algorithms and interface circuits to generate six PWM logic signals. So far researchers mainly concentrated on the development of new control algorithms. However, the cost, simplicity and flexibility of the overall drive system which are some of the most important factors did not get that much attention from the researchers. That is why, despite tremendous research in this area, most of the developed control system failed to attract the industry. Thus, the main issue of this work is to develop a cost effective, simple and efficient high performance PMSM motor drive. Recently, some efforts have been made on the application of FSTPI for variable speed drives. Some advantages of the FSTPI over the conventional SSTPI such as, reduced price due to reduction in number of switches, reduced switching losses, reduced number of interface circuits to supply logic signals for the switches, simpler control algorithms to generate logic signals, less chances of destroying the switches due to lesser contact among switches and less real time computational burden [2]. The invention of high speed power semiconductor devices makes it possible to control the AC drives with SSTPI. This inverter was popular since the last few decades. In recent years, many research and development project focusing the cost reduction of PMSM motor drive had been developed. An AC to AC converter with least amount of hardware was proposed for three phase induction motor (IM) drive. A cost effective FSTPI was proposed for PMSM motor drive. The authors showed a performance comparison of the FSTPI inverter fed drive with SSTPI fed drive in terms of speed response and total harmonic distortion of the stator current. The authors also proposed control scheme for FSTPI PMSM motor drive [23]. A vector control technique for PMSM motor using FSTPI was presented for high

performance industrial drive systems. The authors verified the complete vector control scheme.

Over the year's induction motor (IM) has been utilized as a workhorse in the industry due to its easy build, high robustness, and generally satisfactory efficiency. By tradition, SSTPIs have been widely used for variable speed IM drives [24]. The last work on FSTPI for IM drives investigated the performance of a four-switch three-phase inverter fed cost effective induction motor in real time, which has been implemented by vector control. A standard three-phase voltage source inverter utilizes three legs six-switch three-phase voltage source inverter, with a pair of complementary power switches per phase. The FSTPI structure generates four active vectors in the plane, instead of six, as generated by the SSTPI topology. A reduced switch count voltage source inverter four switch three-phase voltage source inverter uses only two legs, with four switches. Several articles report on FSTPI structure regarding inverter performance and switch control. This presents a general method to generate PWM signals for control of four-switch, three phase voltage source inverters, even when there are voltage oscillations across the two dc-link capacitors. The method is based on the so called space vector modulation, and includes the scalar version. This permits to implement all alternatives, thus allowing for a fair comparison of the different modulation techniques. The proposed method provides a simple way to select either three, or four vectors to synthesize the desired output voltage during the switching period. In the proposed approach, the selection between three or four vectors is parameterized by a single variable .The influence of different switching patterns on output voltage symmetry, current waveform, switching frequency and common mode voltage is examined.

In the FSTPI, they are using in various ways; model-based predictive current control (MBPCC) [15] scheme for FSTPI-fed PMSM motor drive systems based on a three-phase extended back-EMFs estimation method. First, we estimate the three-phase extended back-EMFs of PMSM motor using the information of the stator currents, the *q*-axis inductance, and the stator voltages. After that, the future stator currents are predicted for four possible switching states generated by the FSTPI. By defining a cost function which is related to current errors, one can select a switching state that minimizes the cost function. Then, the future switching state of the FSTPI at the next sampling time can be

determined to directly control the drive signals of FSTPI. In addition, to improve the performance of the closed-loop system, an adaptive back stepping complementary PI sliding-mode (ABCPISM) position controller is proposed. In the performance of a fuzzy logic- controller (FLC)-based cost-effective drive system of PMSM motor for high-performance industrial applications. In this paper, the FLC is used as a speed controller and the motor is fed from a FSTPI PWM inverter instead of a conventional SSTPI. This reduces the cost of the inverter, the switching losses, and the complexity of the control algorithms and interface circuits to generate six PWM logic signals. Furthermore, the proposed control approach reduces the computation for real-time implementation. The closed-loop vector control scheme of the selected FSTPI-fed PMSM motor drive incorporating the FLC is implemented in [24]. A comparison of the FSTPI fed PMSM motor drive with a conventional SSTPI system is also made in terms of performance and harmonic analysis of the stator current. An ADRC based MPCC strategy is developed for PMSM motor fed by FSTPI as an after-fault-topology for fault-tolerant FSTPI. Firstly, the mathematical model of a PMSM motor fed by a FSTPI is built. Then the ADRC and MPCC are respectively designed, with the former being used to realize disturbance estimation and disturbance compensation while the latter being used to reduce stator current ripple and improve the quality of the torque and speed control. The resultant ADRC-based MPCC PMSM motor fed by an unhealthy inverter has fault-tolerant effective with dynamical performance very close to an ADRC-based MPCC PMSM motor fed by a healthy inverter [24, 25, 26]. On the other hand, compared with PI-based MPCC PMSM motor fed by an unhealthy inverter, it possesses better dynamic response behavior and stronger robustness as well as smaller THD index of three-phase stator current in the presence of variation of load torque. The simulation results validate the feasibility and effectiveness of the proposed scheme. A MFPCC for FSTPI-fed PMSM motor drive systems is proposed. A new method, using the stator current and its difference is proposed to predict the next stator current. The advantages of the proposed MFPCC are low computation, simple to realize, and insensitive to parameter variations. The switching state that minimizes a defined cost function, which is used to evaluate the current error at the next switching state, is obtained to control the drive signals of the

FSTPI. Due to its simplicity and powerfulness, the proposed method provides an alternative current controller for the FSTPI - fed PMSM motor drive system.

3.1 Conventional FSTPI voltage source inverter

In FSTPI, two of the output load phases are maintained from the two inverter legs, while the third load phase is fed from the dc-link at the middle point of a split-capacitor bank as shown in Fig. 3.1 Recently, the FSTPI has attracted the most interests regarding its performance, control, and applications [2]. The conventional SSTPI two-level voltage source inverter (VSI) has found widespread industrial applications in different forms such as motor drives, renewable energy conversion systems, and active power filters. However, in some low power range applications, reduced switch count inverter topologies are considered to alleviate the volume, losses, and cost. Some research efforts have been directed to develop inverter topologies that can achieve the aforementioned goal. The results obtained showed that it is possible to implement a three-phase inverter with only four switches. Recently, the FSTPI has attracted the most interests regarding its performance, control, and applications. Compared to the traditional SSTPI, the FSTPI has some advantages such as reduced cost and increased reliability due to the reduction in the number of switches, reduced conduction and switching losses by 1/3, where one entire leg is omitted, and reduced number of interface circuits to supply PWM signals for the switches. The FSTPI can also be utilized in fault tolerant control to solve the open/short-circuit fault of the SSTPI. However, there are some disadvantages of the conventional FSTPI which should be taken into consideration. Similar to the traditional SSTPI, the FSTPI performs only buck dc–ac conversion. Furthermore, the peak phase voltage of the FSTPI is reduced to $\sqrt{3}\,(V_{DC}/2)$, where it is $V_{DC}/2$ in the SSTPI. In order to boost up the phase voltage of the FSTPI to that of SSTPI, the typical solution is to insert a dc–dc boost converter between the dc input source and the FSTPI. However, this adds significant complexity and hardware to the power conversion system and wastes the merits of the reduced switch count. Also, the FSTPI topology is not symmetrical; while two load-phases are directly fed from the two inverter legs, the third load-phase is connected to the center tap of split dc-link capacitors. This forces the current of the third phase to circulate through the dc-link capacitors; hence, a fluctuation will inevitably appear in the two

capacitors' voltages, which correspondingly distorts the output voltage. Moreover, if the dc-link split-capacitors have not equal values, there is a possibility of over modulation of the pulse-width modulation process in order to compensate this dilemma. The SEPIC converter is a fourth-order nonlinear system that is extensively used in step-down or step-up dc–dc switching circuits, photovoltaic maximum power point tracking and power factor correction circuits due to its promising features as the non inverting output voltage buck-boost capability and lower input current ripple content. Based on the aforementioned advantages, SEPIC converter has been recently researched by scholars in various topologies in many diversified studies. Although the proposed FSTPI SEPIC inverter has not a voltage boost capability, it can produce an output voltage higher than that of the conventional FSTPI VSI by a factor of two, which improves the voltage utilization factor of the input dc supply. Another attractive feature of the proposed SEPIC inverter is that the output voltage is a pure sinusoidal wave, therefore reducing the filtering requirements at the output stage. Also, there is no vital need to insert a dead-band between the same-leg switches, which significantly reduces the output waveform distortion and gain nonlinearity.

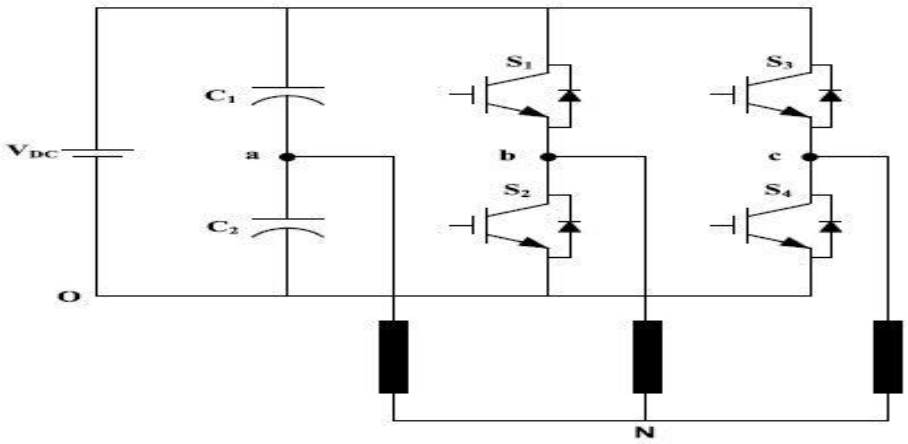

Fig. 3.1 Conventional FSTPI voltage source inverter.

3.2 Sliding Mode Control (SMC)

Sliding mode controller (SMC) is a kind of nonlinear controller which was introduced for controlling variable structure systems (VSS). Its major advantages are

guaranteed stability and robustness against parameter, line, and load uncertainties. Moreover, being a controller that has a high degree of flexibility in its design choices, the SM controller is relatively easy to implement as compared to other types of nonlinear controllers. Such properties make it highly suitable for control applications in nonlinear systems, including power electronics. It has been repeatedly demonstrated that the SMC controller is a viable solution for enhancing the control performance of power converters [27].

SMC is a nonlinear control theory which extends the properties of hysteresis control to multivariable environments. It is able to constrain the system status to follow trajectories which lie on a suitable surface in the state space (the sliding surface). The main advantages of SMC are the fast dynamic response and the guarantee of stability and robustness for large variations of system parameters and against perturbations. Moreover, given its flexibility in terms of synthesis, SMC is relatively easy to be implemented compared to other types of nonlinear control. However, its application to power converters should be studied for each converter severally. As a control method, SMC has been applied to basic dc–dc converters and complex converters. Although most authors mention the generalization of their developed methods to other high-order converters, this does not imply to all converters because the difference in circuit topology completely changes the system's behavior even if it is of the same order.

3.2.1 Sliding Surface

Although the output voltage v_{C2} of each single-ended primary inductance converter (SEPIC) is the final control target, it will be impossible for the closed-loop controlled system to reach stable motion on the sliding surface if v_{C2} is only selected to be the direct control target, thus the other variables should be chosen. Then, it is proposed to increase the number of state variables as low as possible in the sliding surface. To avoid a large number of tuning gains, a surface containing the input current in addition to the output voltage could be chosen as given by Eqn. 3.1

$$S\,(i_{L1},\, v_{C2}) = \alpha_1 e_1 + \alpha_2 e_2 \tag{3.1}$$

Where coefficients α_1 and α_2 are gains, while e_1 and e_2 are the feedback errors of the state variables i_{L1}, and v_{C2}, respectively, and given by Eqn. 3.2

$$e_1 = i_{L1\text{ref}} - i_{L1}$$
$$e_2 = v_{C2\text{ref}} - v_{C2} \tag{3.2}$$

The reason for choosing i_{L1} instead of i_{L2} is to allow the sliding surface to directly control the input of each converter in addition to its output, which is more stable than the other cases. At an infinitely high switching frequency, the SMC will ensure that both input inductor current and output capacitor voltage are regulated to follow exactly their instantaneous references i_{L1ref} and v_{C2ref}, respectively. However, in the case of finite frequency or fixed frequency SMCs, the control is imperfect, where steady-state errors exist in both inductor current and output capacitor voltage. A good method for suppressing these errors is to introduce an additional integral term of the state variables into the sliding surface. Therefore, an integral term of these errors is introduced into the SMC as an additional controlled state-variable to reduce these steady-state errors. This is commonly known as integral sliding-mode control (ISMC) [28, 2], and the sliding surface are selected as specified by Eqn 3.3.

$$s = \alpha_1 e_1 + \alpha_2 e_2 + \alpha_3 e_3 \tag{3.3}$$

where, α_1 , α_2 , and α_3 represent the desired control parameters denoted sliding coefficients, while e_1 ,e_2 and e_3 are expressed as

$$\begin{aligned} e_1 &= i_{L1\text{ref}} - i_{L1} \\ e_2 &= v_{C2\text{ref}} - v_{C2} \\ e_3 &= \int (e_1 + e_2) dt \end{aligned} \tag{3.4}$$

The time derivative of the three-state errors is given by

$$\begin{aligned} \frac{de_1}{dt} &= \frac{d(i_{L1ref} - i_{L1})}{dt} \\ \frac{de_2}{dt} &= \frac{d(v_{C2ref} - v_{C2})}{dt} \\ \frac{de_3}{dt} &= e_1 + e_2 \end{aligned} \tag{3.5}$$

The inductor current reference is difficult to evaluate as it has a nonconventional form and generally depends on the load power demand, supply voltage, and load voltage. In practical implementation, the state variable error for the inductor current is obtained from the actual current either by using a high-pass filter to obtain the inductor current ripples at the switching frequency that simulates the error, or by using a low-pass filter to pass only the fundamental component of the inductor current then the actual current is subtracted from this reference signal to get the state error. To avoid increasing the system order and altering the converter dynamics when such filters are used, the inductor current reference can be chosen as

$$i_{L1\text{ref}} = K\,(v_{C2\text{ref}} - v_{C2}) \tag{3.6}$$

where K is an amplifying gain of the converter output voltage error. Substituting Eqn. 3.5 in Eqn. 3.6 gives

$$\frac{d_{e1}}{dt} = \frac{d(i_{L1ref} - i_{L1})}{dt} = \frac{d[K(v_{C2ref} - v_{C2})}{dt} \tag{3.7}$$

Considering the time derivative of the output capacitor voltage

$$\frac{d_{vc2}}{dt} = \frac{i_{c2}}{c_2} \tag{3.8}$$

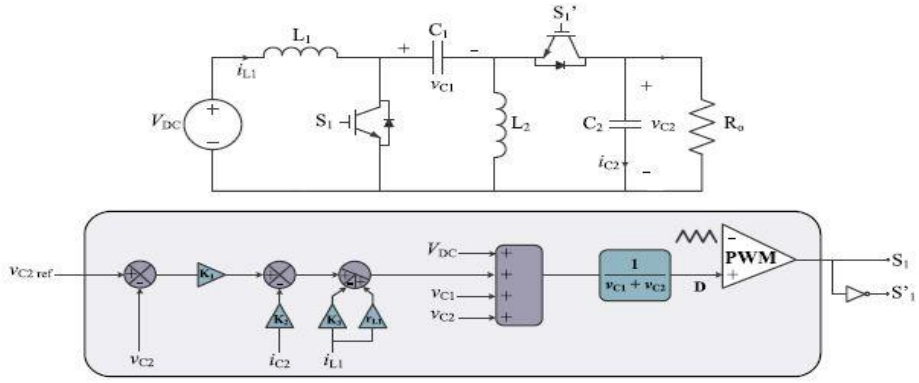

Fig. 3.2 ISMC for SEPIC converter

To simplify the calculation, assuming that $v_{C2\text{ref}}$ is constant, and substituting equation (15) [2] and Eqn. 3.8 in Eqn. 3.7 gives

$$\frac{d_{e1}}{dt} = \frac{-K}{C_2} i_{c2} - [\frac{(D-1)(v_{c1} + v_{c2})}{L_1} - \frac{r_{L1}}{L_1} i_{L1} + \frac{V_{DC}}{L_1}]$$

$$\frac{d_{e1}}{dt} = \frac{d(v_{C2ref} - v_{C2})}{dt} = \frac{-i_{C2}}{C_2}$$

$$\frac{d_{e3}}{d_t} = e_1 + e_2 = (K+1)(v_{C2ref} - v_{C2}) - i_{L1} \tag{3.9}$$

where D is the equivalent control signal denoted as the duty cycle of the converter, which could be formulated using the invariance conditions by setting the time derivative of Eqn. 3.3 to zero as follows [50]:

$$\frac{ds}{dt} = \alpha_1 \frac{de_1}{dt} + \alpha_2 \frac{de_2}{dt} + \alpha_3 \frac{de_3}{dt} = 0 \tag{3.10}$$

Solving for the equivalent control signal yields

$$D = \frac{1}{v_{C1} + v_{c2}} [K_1(v_{C2ref} - v_{C2}) - K_2 i_{C2} - K_3 i_{L1} + r_{L1} i_{L1} + (v_{C1} + v_{C2} - V_{in})] \tag{3.11}$$

Where $K_1 = \frac{\alpha_3}{\alpha_1} L_1(K+1)$, $K_2 = \frac{L_1}{C_2}(K + \frac{\alpha_2}{\alpha_1})$ and $K_3 = \frac{\alpha_3}{\alpha_1} L_1$ are the fixed gain parameters of the recommended ISMC. The block diagram of the ISMC given by is illustrated in Fig. 3.3.

3.2.1.1 Double-Integral Sliding-Mode Control (DISMC)

To increase the effectiveness of the ISMC, an additional double-integral term of the state-variables error could be introduced in the sliding surface. This is the so-called DISMC [2]. Thus, the DISM controller has the following sliding surface

$$s = \alpha_1 e_1 + \alpha_2 e_2 + \alpha_3 e_3 + \alpha_4 e_{4b} \tag{3.12}$$

Where the state errors are defined by

$$e_1 = i_{L1\text{ref}} - i_{L1}$$
$$e_2 = v_{C2\text{ref}} - v_{C2}$$
$$e_3 = \int (e_1 + e_2)dt$$
$$e_4 = \iint e_1 dt \tag{3.13}$$

Substituting the SEPIC state-space models under CCM into the time derivative of Eqn. 3.13 gives the dynamical model of the system as

$$\frac{de_1}{dt} = \frac{-K}{C_2} i_{C2} - [\frac{(D-1)(v_{C1} + v_{C2})}{L_1} - \frac{r_{L1}}{L_1} i_{L1} + \frac{V_{DC}}{L_1}$$
$$\frac{de_2}{dt} = \frac{d(v_{C2ref} - v_{C2})}{dt} = \frac{-i_{C2}}{C_2}$$
$$\frac{de_3}{dt} = e_1 + e_2 = (K+1)(v_{C2\text{ref}} - v_{C2}) - i_{L1}$$
$$\frac{de_4}{dt} = \int e_1 dt \tag{3.14}$$

The equivalent control signal deduced from setting the time derivative of Eqn. 3.12 into zero gives

$$D = \frac{1}{v_{C1} + v_{c2}} [K_1(v_{C2ref} - v_{C2}) - K_2 i_{C2} - K_3 i_{L1} + r_{L1} i_{L1} + (v_{C1} + v_{C2} - V_{in})] + \int K_4 (v_{C2ref} - v_{C2}) dt) \tag{3.15}$$

Where $K_1 = \frac{\alpha_3}{\alpha_1} L_1 (K+1)$, $K_2 = \frac{L_1}{C_2}(K + \frac{\alpha_2}{\alpha_3})$, $K_3 = \frac{\alpha_3}{\alpha_1} L_1$ and $K_4 = \frac{\alpha_4}{\alpha_1} L_1$ are the fixed gain parameters in the recommended DISM controller. Eqn. 3.15 Shows that the DISMC introduces an integral term of the capacitor voltage error component in the equivalent control, which allows solving the problem of the significant steady-state errors in the ISMC algorithm. The block diagram of the DISMC given by Eqn. 3.15 is illustrated in Fig. 3.3.

3.2.1.2 Selection of DISM Control Parameters

The system behavior is completely determined by coefficients Ki, which must be selected so as to satisfy the existence condition of the SMC and ensure stability and fast response even for large supply and load variations. The existence condition for the SMC consists of finding the regions of attraction given by $s(x)\frac{ds(x)}{dx} < 0$ throughout the entire domain of operation which are imposed by the SMC strategy. These regions are found using the following inequalities [2]:

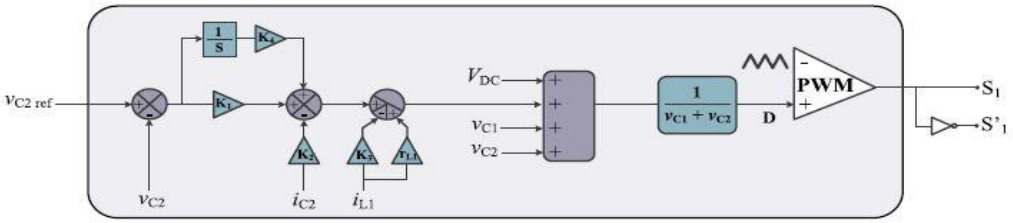

Fig. 3.3 DISMC for SEPIC converter

$$\begin{cases} u = 1, & \frac{ds(x)}{dx} < 0, \text{ if } s(x) > 0 \\ u = 0, & \frac{ds(x)}{dx} > 0, \text{ if } s(x) < 0 \end{cases} \tag{3.16}$$

Detailing equation (3.16) leads to

Case 1: $s(x) > 0$, u=1, then $\frac{ds(x)}{dx} < 0$,

$$V_{in} - K_1(v_{C2ref} - v_{C2}) - \int K_4(v_{C2ref} - v_{C2})dt + K_2 i_{C2} - (K_3 - r_{L1})i_{L1} > 0 \tag{3.17}$$

Case 1: $s(x) < 0$, u=0, then $\frac{ds(x)}{dx} > 0$

$$V_{in} - K_1(v_{C2ref} - v_{C2}) - \int K_4(v_{C2ref} - v_{C2})dt + K_2 i_{C2} - (K_3 - r_{L1})i_{L1} < v_{C1} + v_{C2} \tag{3.18}$$

Since existence conditions are expressed by inequalities Eqn. 3.17, there are some degrees of freedom in choosing coefficients *Ki*. The solutions giving stable and non oscillatory response of all state variables can therefore be investigated. This can be obtained by finding the system Eigen values as a function of the coefficients *Ki* in order

to find the solutions having Eigen values with negative real part and suitable dynamic behavior.

3.2.1.3 Parameters and ratings selection for SEPIC inverter components

I. Inductors Selection

Retrieving equation 1 [2], the relation between input, and output voltages and currents for SEPIC converter is as follows:

$$\frac{i_{in}(t)}{i_o(t)} = \frac{v_o(t)}{V_{DC}} = \frac{D(t)}{1-D(t)} \tag{3.19}$$

where $D(t)$ is the instantaneous duty cycle, which can be expressed by (34)

$$D(t) = \frac{v_o(t)}{V_{DC} + v_o(t)} \tag{3.20}$$

Considering the first converter in the proposed SEPIC inverter topology, which is connected to phase B, and retrieving equations Eqn. 2 and Eqn. 6 [2], i.e., $v_{BO}(t) = V_{DC} - V_{mL-L} \sin(\omega t)$ and $i_B(t) = I_m \sin(\omega t - \emptyset - 5\pi/6)$. Then, the instantaneous duty for the first converter is calculated as follows

$$D(t) = \frac{V_{DC} - V_{mL-L}\sin(\omega t)}{2V_{DC} - V_{mL-L}\sin(\omega t)} \tag{3.21}$$

To find the duty cycle at the highest output current, it is necessary to find the time at which the current becomes at its peak value. For the load current $i_B(t)$, it will be at the level of I_m when

$$\omega t = \frac{4\pi}{3} + \phi \tag{3.22}$$

Then, the duty cycle correspondent to this maximum current is $\hat{D}$, and could be found as follows

$$D_{atI_m} = \hat{D} = \frac{V_{DC} - V_{mL-L}\sin(4\pi/3 + \phi)}{2V_{DC} - V_{mL-L}\sin(4\pi/3 + \phi)} \tag{3.23}$$

It is clear from Eqn. 3.22 that the highest possible duty cycle occurs at $\phi = \pi/6$, which is not depending on the ratio of (V_{mL-L}/V_{DC}). The corresponding maximum duty cycle

could be found by Eqn. 3.23, and will be used in design which emulates the worst possible case

$$D_{\max conv1} = \frac{V_{DC} - V_{mL-L}}{2V_{DC} - V_{mL-L}} \tag{3.24}$$

For the second converter in the proposed SEPIC inverter topology, which is connected to phase C, i.e., $v_{CO}(t) = V_{DC} + V_{mL-L} \sin(\omega t + 2\pi/3)$ and $i_C(t) = i_m \sin(\omega t + \pi/2 - \phi)$. The instantaneous duty cycle is calculated as follows:

$$D(t) = \frac{V_{DC} + V_{mL-L} \sin(\omega t + 2\pi/3)}{2V_{DC} + V_{mL-L} \sin(\omega t + 2\pi/3)} \tag{3.25}$$

For the load current $i_C(t)$, it will be at the level of I_m when

$$\omega t = \phi \tag{3.26}$$

Then, the duty cycle correspondent to this maximum current is $\hat{D}$, and could be found as follows:

$$D_{atI_m} = \hat{D} = \frac{V_{DC} + V_{mL-L} \sin(2\pi/3 + \phi)}{2V_{DC} + V_{mL-L} \sin(2\pi/3 + \phi)} \tag{3.27}$$

It is clear from Eqn. 3.27 that the highest possible duty cycle, at the peak current, occurs at $\phi = 0$, regardless of the ratio of (V_{mL-L}/V_{DC}). The corresponding maximum duty cycle is given by Eqn. 3.28, and will be used in design which emulates the worst possible case

$$D_{\max conv2} = \frac{V_{DC} + (\sqrt{3}/2)V_{mL-L}}{2V_{DC} + \sqrt{3}/2V_{mL-L}} \tag{3.28}$$

1) **Input Inductor Selection**: Considering that the peak-to peak ripple current through the input inductor is set to 10% of the maximum value of the converter input current. The input inductor ripple current can be expressed as

$$\Delta_{iL1\max} = 10\% \text{ of input current peak} = 0.1 I_m \frac{D_{\max}}{1 - D_{\max}} \tag{3.29}$$

Also, from the dc–dc converter basics, the ripple current can be expressed as

$$\Delta i_{L\max} = \frac{V_{DC} D_{\max}}{L f_{sw}} \tag{3.30}$$

where *fsw* is the switching frequency, while L is the inductance value. Equating Eqn. 3.28 and Eqn. 3.29, the input inductance L_1 is estimated as in Eqn 3.30.

$$L_1 = \frac{V_{DC}(1 - D_{\max})}{0.1 I_m f_{sw}} \tag{3.31}$$

2) Output Inductor Selection: For the output inductor, the peak-to-peak ripple current is recommended to be 30% of the maximum value of the converter output current [51]. Following the same steps used in the selection of the input inductor, L_2 could be selected according to the following equation:

$$L_2 = \frac{V_{DC} D_{\max}}{0.3 I_m f_{sw}} \tag{3.32}$$

II. Capacitances Selection

1) **Coupling Capacitor Selection**: Based on the desired voltage ripples, the capacitance can be selected as follows:

$$C_1 = \frac{I_m D_{\max}}{\Delta V f_{sw}} \tag{3.33}$$

The ripple voltage across the coupling capacitance ΔV is recommended as 5% of the dc input voltage (VDC).

2) **Output Capacitor Selection**: The design Eqn. 3.32 is typically used for the selection of the output capacitor. The only change is that the ripple voltage across the output capacitor

Inductors	$L_{1B} = 6.77mH$, $L_{2B} = 2.26mH$
	$L_{1C} = 7mH$, $L_{2C} = 2.36mH$,
Capacitors	$C_{1B} = 10.6\mu F$, $C_{2B} = 2.8\mu F$
	$C_{1C} = 10.3\mu F$, $C_{2C} = 2.8\mu F$
DISMC coefficients	$K_1 = 2$, $K_2 = 10$, $K_3 = 1$, $K_4 = 100$,

Table. 3.1 Parameters of FSTPI SEPIC inverter

Δ_{Vo} is recommended to be 10% of the peak voltage applied on the output of the SEPIC, which is equal to $V_{DC} + V_{mL-L}$. The output capacitor is selected according to Eqn. 3.34.

$$C_2 = \frac{I_m D_{\max}}{\Delta V_O f_{sw}} \tag{3.34}$$

III. Ratings of Switching Devices

For the proposed inverter topology, the voltage stresses of all switching devices for each SEPIC are equal to the sum of the input voltage and maximum output voltage as follows:

$$V_{Dmax} = V_{SWmax} = V_{DC} + V_{mL-L} \tag{3.35}$$

where V_D and V_{SW} are the voltage across the diode and the switch, respectively. Also, the maximum stresses I_{Dmax} and I_{SWmax} of the diodes and switches could be deduced from as follows:

IV. Design Example

In this section, the previously deduced equations are used to select the appropriate values of the components used in the proposed SEPIC inverter [2].

The design specifications of the proposed FSTPI SEPIC inverter are as follows:

1) input voltage: 200 V_{DC};

2) Peak output line voltage: $100\sqrt{3}$ V_{AC};

3) Output frequency: 50 Hz;

4) Switching frequency: 25 kHz;

5) Rated current: Im = 4A (Load: 25 Ω series with 1mh). From Eqn. 3.24, $D_{\max\ conv1}$ = 0.65, while from Eqn. 3.25, $D_{\max\ conv2}$ = 0.63. The parameters of both SEPIC converters for the above mentioned specifications are summarized in Table 3.1.

After the verification of all the performance of the FSTPI SEPIC inverter, Fig. 3.4 shows the performance of the inverter during normal operating conditions, where the output capacitor voltage and the coupling capacitor voltage of both SEPIC converters are shown in Fig. 3.4(a) and (b), respectively. Fig. 3.4(a) shows that the output voltages of both SEPIC converters have sinusoidal waveforms shifted by 120° with a dc bias that is exactly equal to the input dc voltage. Fig. 3.4(b) shows that the average value of the coupling capacitor voltage for both SEPIC converters is equal to the value of the input dc voltage. The current of both input and output inductors for each SEPIC converter is show

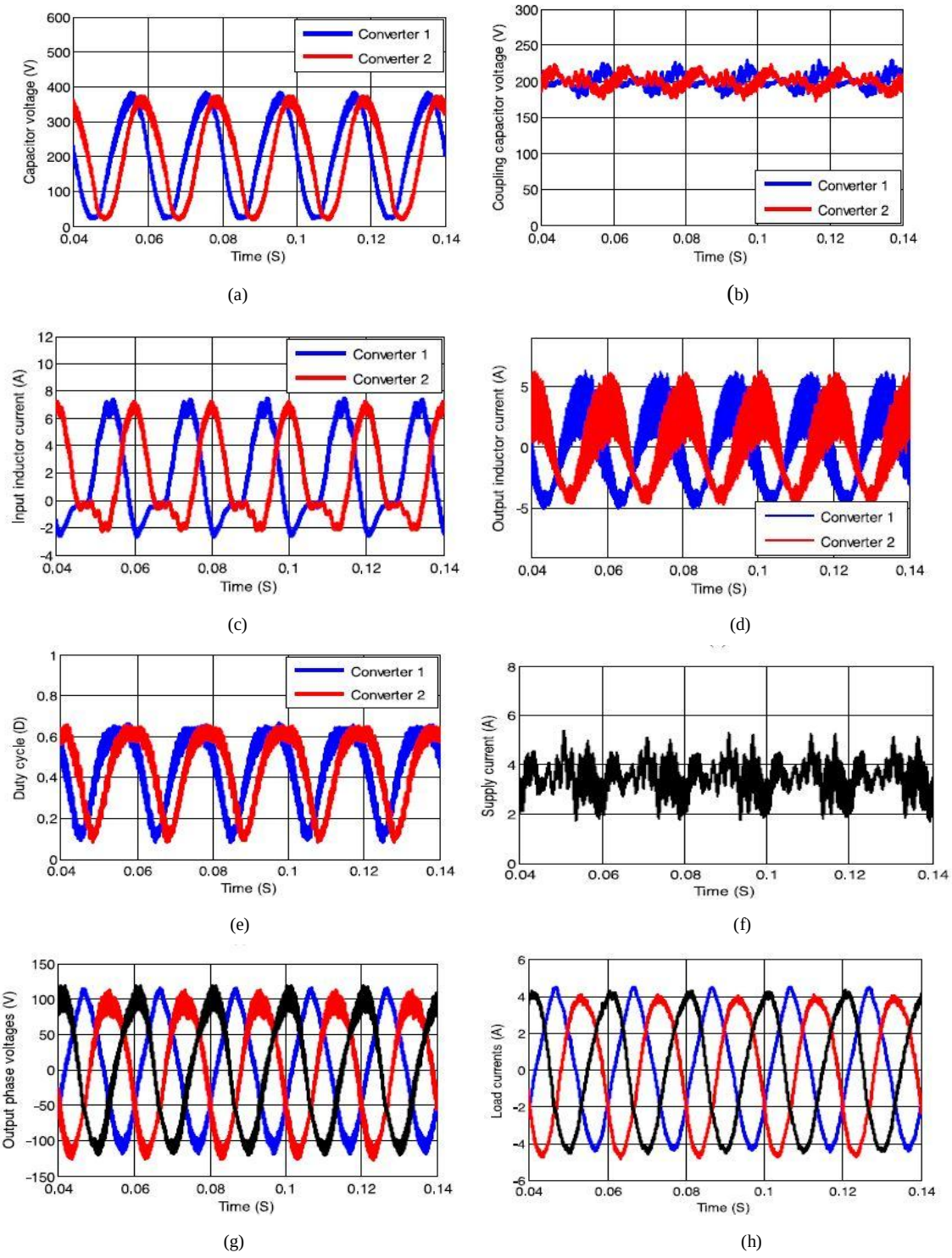

Fig. 3.4 Performance of the FSTPI SEPIC inverter under normal operating conditions (a) Output capacitor voltage of both SEPIC converters. (b) Coupling capacitor voltage of both SEPIC converters. (c) Input inductor current of both SEPIC converters. (d) Output inductor current of both SEPIC converters. (e) Duty cycle of both SEPIC converters. (f) Dc supply current. (g) Three-phase output voltages. (h) Three-phase load currents.

in Fig. 3.4(c) and (d), respectively. Fig. 3.4(c) shows that the simulated waveforms of the input inductor currents for both SEPIC converters. Fig. 3.4(d) shows that the output inductor current has the same waveform of the corresponding load current with superimposed switching ripples. The duty cycle of both SEPIC converters is shown in Fig. 3.4(e), where they are varying between approximately 0.12 and 0.65. It should be noted that the waveform of the duty cycle of the SEPIC converter is similar to that obtained from the buck-boost converter at the same values of input and output voltages. This is due to the fact that both SEPIC and buck-boost converters have the same magnitude of the input/output relationship. The input current of the dc supply is shown in fig. 3.4(f). This oscillation is due to the ripples imposed on the input inductor current of both SEPIC, and ripples of phase-A current. The three-phase output voltages and load currents of the inverter are shown in Fig. 3.4(g) and (h), respectively, where the output voltages are well regulated without any filtering requirements [2].

CHAPTER-4

FSTPI Inverter Fed PMSM drive

In this chapter the control of PMSM motor through four switch inverter is explored. PMSM motor is typically used for high-performance and high efficiency motor drives. High-performance characterized by smooth rotation over the entire speed range of the motor, full control at zero speed, and fast acceleration and deceleration, are achieved. For FSTPI FOC [3, 10], DTC [5, 11] and MPC [15, 10] control techniques are being widely used. FSTPI is usually adopted as the topology for continuous fault-tolerant operation of a Direct Torque (DTC) system when inverter fault occurs [5]. Due to that the FSTPI can only provide four voltage space vectors with unequal amplitude, the DTC system performance will deteriorate to a certain extent. To enhance the performance of PMSM motor drive fed by FSTPI, a sliding mode controller with the analysis and design of the controller included is proposed for the purpose of direct control of the torque and stator flux linkage. Besides a nonlinear perpendicular flux observer is adopted to estimate the stator flux more accurately as well.

A FSTPI [2] has been selected as a promising inverter design to reduce the cost, complexity, size, and switching losses of the dc–ac conversion system. Traditional FSTPI usually operates at half the dc input voltage; hence, the output line voltage cannot exceed this value. The selected topology provides pure sinusoidal output voltages with no need for output filter. Compared to previous FSTPIs, this FSTPI improves the voltage utilization factor of the input dc supply, where this topology provides higher output line voltage which can be extended up to the full value of the dc input voltage. The integral sliding-mode control is used with this topology to optimize its dynamics and to ensure robustness of the system during different operating conditions. The components ratings are derived for the parameters in the [2].

Over the last two decades, the PMSM motor has been paid much attention for variable speed drive (VSD) systems due to its high torque to current ratio, large power to weight ratio, high efficiency, high power factor and robustness. With the invent of high speed power semiconductor devices three-phase inverters play the key role for variable

speed ac motor drives. Traditionally, SSTPI have been widely used for variable speed PMSM motor drives. These inverters have some drawbacks, which involve the losses of the six switches as well as the complexity of the control algorithms and interface circuits to generate six PWM logic signals. Recently, some efforts have been made on the application of FSTPI to uninterrupted power supplies and variable speed drives**.**

Most of the reported works on FSTPI for machine drives did not consider the closed loop vector control scheme, which is essential for high performance drives. Usually, high performance motor drives used in robotics, rolling mills, machine tools, etc. require fast and accurate response, quick recovery of speed from any disturbances and insensitivity to parameter variations. The dynamic behavior of an ac motor can be significantly improved using vector control theory where motor variables are transformed into an orthogonal set of *d-q* axes such that speed and torque can be controlled separately [29]. Most of the past research on variable speed PMSM motor drives mainly concentrated on the development of the efficient control algorithms high performance drives. However, the cost, simplicity and flexibility of the overall drive system which become some of the most important factors did not get that much attention to the researchers. That is why, despite tremendous research in this area most of the developed control system failed to attract the industry. Thus, the main issue is to develop a cost effective, simple and efficient high performance PMSM motor drive system.

In this work, a PMSM motor with parameters from [30] and FSTPI are used for simulation. The circuit is given in Fig. 4.1. The simulation results are displayed in Fig. 4.5.

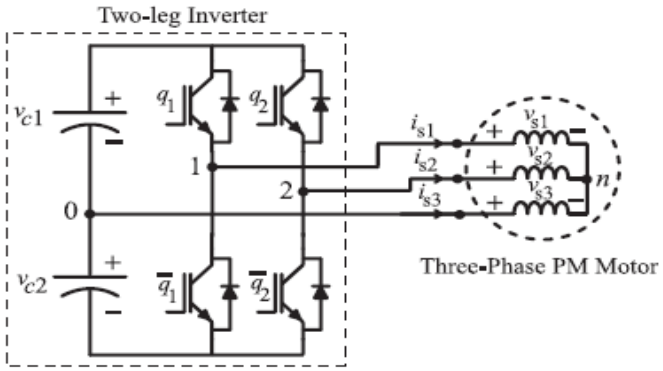

Fig. 4.1 Schematic diagram of FSTPI fed PMSM Motor.

PMSM motors are widely used because they have many advantages such as rugged construction, easy maintenance, high efficiency, and high power factor. However, the most important problems are cost and reliability of the drive system: power electronics, digital processors and effective control algorithms. These problems restrained spreading of the PMSM motor based drives in the field of low-cost applications such as automotive and home appliance.

There are many PMSM motor drive schemes have been researched [30, 31]. These PMSM motor are usually fed by SSTPI. However, they have drawbacks in view of cost. They are relatively expensive because they need six switches and corresponding gate drive circuits. Hence, the schemes using FSTPI have been widely researched for cost reduction by the elimination of power switches and additional circuits such as gate drives. From that point of view the main algorithm for PMSM motor drives is position and speed estimation algorithm for vector sensorless control system. In most PMSM motor drives, some types of shaft sensor such as an optical encoder or a resolver are connected to the rotor shaft. However, such sensors cause several disadvantages such as drive cost, reliability, machine size, and noise immunity. Hence, the speed and position sensorless control has been desired. Among many sensorless control schemes, there are studies taking an approach to the design of closed-loop observers.. A closed-loop vector control scheme of the proposed FSTPI fed PMSM motor drive is simulated using the MATLAB - SIMULINK. A comparison of the proposed FSTPI fed PMSM motor drive with a conventional SSTPI system is also made in terms of performance analysis. This control method verifies the validity of an FSTPI fed PMSM motor drive system for cost reduction and other advantages such as reduced switching losses, reduced number of interface circuits to supply logic signals for the switches, easier control algorithms to generate logic signals.

4.1 Modeling of PMSM

The complete drive system modeling involves the modeling of the PMSM motor, inverter and the controller, which are discussed in the following subsections. Over the years, traditionally, SSTPI have been widely utilized for variable speed alternating current (ac) motor drives. Recently, some efforts have been made on the application of

FSTPI for uninterruptible power supply and variable speed drives. This is due to some advantages of the FSTPI over the conventional SSTPI such as reduced price due to reduction in number of switches, reduced switching losses, reduced number of interface circuits to supply logic signals for the switches, simpler control algorithms to generate logic signals, less chances of destroying the switches due to lesser interaction among switches, and less real-time computational burden. However, most of the Four-switch three-phase inverters are limited to induction motor and BLDC motor systems reported the application of a FSTPI for BLDC motor system in which an open-loop PWM control scheme is considered. Moreover, due to the absence of magnetic saliency, the control of a BLDC motor is much easier than that of the PMSM motor, which is considered in this work. Reported works on the FSTPI for machine drives did not adequately consider the closed-loop vector control scheme utilized a FSTPI for closed-loop vector control of induction motor, where the proportional–integral (PI) algorithm was used for speed and current control purposes. The disadvantage of the PI algorithm is well known due to its dependence on machine parameters [24, 31]. Furthermore, the reported works on FSTPI did not adequately investigate the dynamic performances of the drive, although it is one of the main concerns for high-performance drive applications. Thus, a FLC is utilized to replace the PI controller. Despite a lot of advantages of FLC over the conventional PI controllers [23], the real-time implementation of an FLC in motor drive suffers from high computational burden. In such a case, the proposed FSTPI inverter will be a good candidate to minimize some computational burden in real time. Nowadays, the PMSM is becoming popular for variable speed- drive systems due to its high torque-to-current ratio, large power-to-weight ratio, high efficiency, high power factor, and robustness. The precise speed control of a PMSM motor drive becomes a complex issue due to nonlinear coupling among its winding currents and the rotor speed as well as the nonlinearity present in the electromagnetically developed torque due to magnetic saturation of the rotor core. Most of the past research on variable speed PMSM motor drives mainly concentrated on the development of the efficient control algorithms for high performance drives. However, cost, simplicity, and flexibility of the overall drive system, which are some of the most important factors, did not get that much attention to the researchers. Despite tremendous research in this area, most of the developed control systems failed to

attract attention of the industry. In the past, researchers also applied multilevel inverter system for high power applications. Again, this system involves more losses and complex switching, if the inverter is not required for that power level. Thus, one of the main points of this is to develop a cost-effective, simple, and efficient high-performance PMSM motor drive. High-performance motor drives used in robotics, rolling mills, machine tools, etc. require fast and accurate response, quick recovery of speed from any disturbances as well as insensitivity to parameter variations. The dynamic behavior of an ac motor can be significantly improved using vector control theory, where motor variables are transformed into an orthogonal set of *d–q* axes such that speed and torque can be controlled separately. This gives the PMSM motor machine the highly desirable dynamic performance capabilities of a separately excited dc machine while maintaining the general advantages of ac over dc motors.

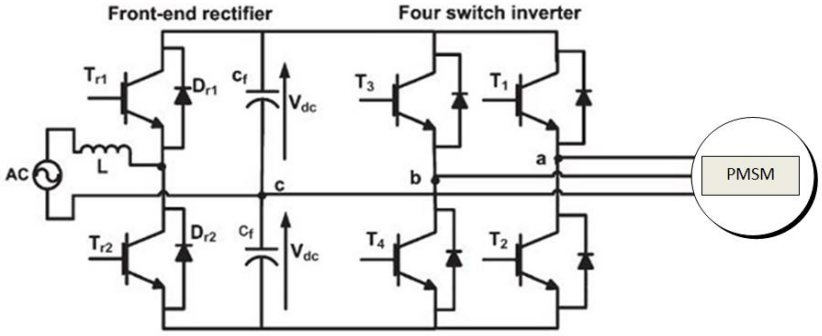

Fig. 4.2 FSTPI fed PMSM motor.

This presents an FLC-based FSTPI-fed cost effective PMSM motor drive system for high performance industrial applications. In order to verify the robustness of the proposed approach, the performance of the proposed drive is investigated both theoretically and experimentally at different operating conditions. A comparison of the proposed FSTPI fed PMSM motor drive with a conventional SSTPI is also made in terms of THD of the stator current and speed response [33]. The FSTPI-fed PMSM drive is found reasonably good considering its performance, cost reduction, and other inherent advantageous features.

4.1.1 Modeling of the drive system

The complete drive system modeling involves the modeling of the inverter, PMSM motor, and controllers, which are discussed in the following.

1. Rectifier–Inverter Operation

The power circuit of the PMSM motor fed from FSTPI voltage source inverter is shown in Fig. 4.2. The circuit consists of two parts. The first part is a front-end rectifier powered from single phase supply. The single-phase ac input, which is of fixed frequency, is rectified by the front-end rectifier switches *T*r1 and *T*r2. The split capacitor bank in the dc link is charged through the diodes associated with *T*r1 and *T*r2. The switches *T*r1 and *T*r2 are operated on a PWM pattern synchronized to the ac mains to shape input current to be sinusoidal. The inductor *L* helps in filtering the higher order current harmonics. The synchronized PWM (SPWM) technique is used to eliminate several lower order harmonics and to control the operation of switches T_{r1} and T_{r2}. The front-end rectifier is also controlled to ensure unity input power factor at the supply side [24, 35, 36].

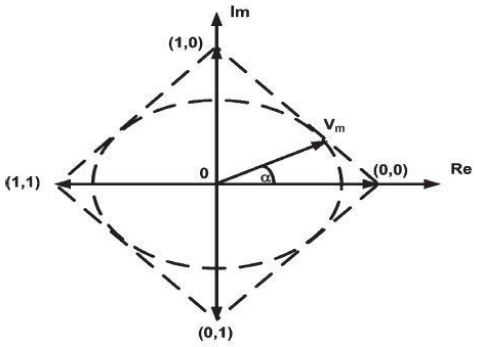

Fig. 4.3 Switching vectors for a FSTPI.

The second part is the FSTPI. Two phases "*a*" and "*b*" are connected through two legs of the inverter, while the third phase is connected to the center point of the dc-link capacitors C_1 and C_2. The four-switch inverter employs four switches and four diodes to operate two line-to-line voltages V_{cb} and V_{ac}, whereas V_{ba} is generated according to Kirchhoff's voltage law from a split capacitor bank. The maximum obtainable peak value of the voltage across each capacitor equals V_{dc}.

Switching function		Switch on		Output voltage vector		
Sa	Sb			Va	Vb	Vc
0	0	T2	T4	-Vdc/3	-Vdc/3	2Vdc/3
0	1	T2	T3	Vdc	Vdc	-2Vdc
1	0	T1	T4	Vdc/3	Vdc/3	-3Vdc/3
1	1	T1	T3	Vdc/3	Vdc/3	-2Vdc/3

Table 4.1 Inverter modes of operation

The inverter switches are considered as ideal switches in the analysis. The output voltages are defined by the gating signals of the two leg switches and by the two dc-link voltages V_{dc}. The phase voltage equations of the motor can be written as a function of the switching logic of the switches and the dc-link voltage. These are given as

$$V_a = \frac{V_{dc}}{3}[4S_a - 2S_b - 1] \tag{4.1}$$

$$V_b = \frac{V_{dc}}{3}[-4S_b - 2S_a - 1] \tag{4.2}$$

$$V_c = \frac{V_{dc}}{3}[-4S_a - 2S_b + 1] \tag{4.3}$$

Where,

V_a, V_b,V_c motor phase voltages;

V_{dc} voltage across the dc-link capacitors;

S_a, S_b switching function for each phase leg.

In matrix form, the above equations can be written as

$$\begin{bmatrix} V_a \\ V_b \\ V_c \end{bmatrix} = \frac{V_{dc}}{3}\begin{bmatrix} 4 & -2 \\ -2 & 4 \\ -2 & -2 \end{bmatrix}\begin{bmatrix} S_a \\ S_b \end{bmatrix} + \frac{V_d}{3}\begin{bmatrix} -1 \\ -1 \\ 2 \end{bmatrix} \tag{4.4}$$

4.1.2 PMSM Model

The mathematical model of a PMSM motor drive can be described by the following equations in a synchronously rotating rotor *d–q* reference frame as [24]:

$$L_q \frac{di_q}{dt} = v_q - Ri_q - P\omega_r L_d i_d - P\omega_r \psi_f$$

$$L_d \frac{di_d}{dt} = v_d - Ri_d - P\omega_r L_q i_q$$

$$\begin{bmatrix} V_d \\ V_q \end{bmatrix} = \begin{bmatrix} R + \rho L_d & -P\omega r L_q \\ P\omega r L_d & R + \rho L_q \end{bmatrix} \begin{bmatrix} i_d \\ i_q \end{bmatrix} + \begin{bmatrix} 0 \\ P\omega r \psi f \end{bmatrix} \tag{4.5}$$

$$T_e = T_L + J_m p\omega_r + B_m \omega_r$$
$$T_e = \frac{3P}{2}(\psi_f i_q + (L_d - L_q) i_d i_q). \tag{4.6}$$

It is well known that a synchronous motor is unable to self-start when supplied with a constant frequency source. The starting torque of the PMSM motor used in this research is provided by a rotor squirrel cage winding.

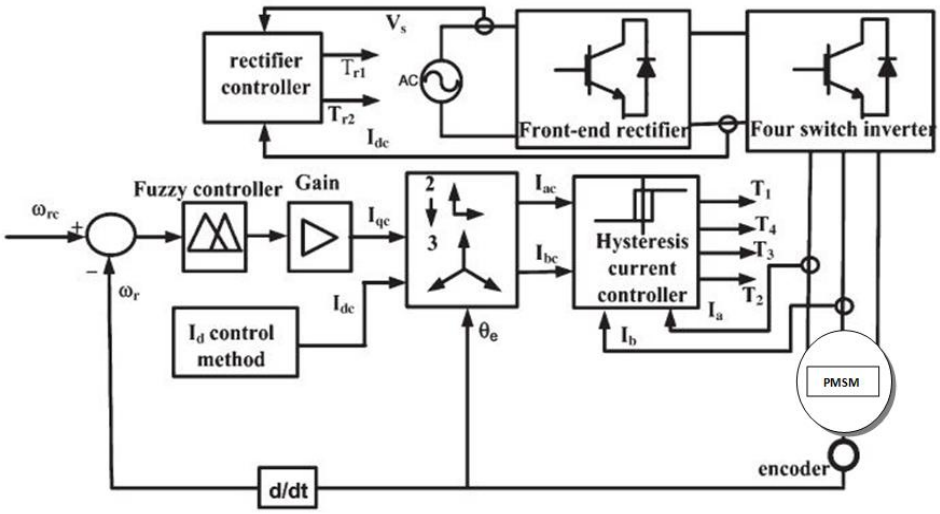

Fig. 4.4 Control setup for a PMSM motor drive.

The starting process of the PMSM motor drive can be considered as a superposition of two operating modes, namely: 1) unsymmetrical asynchronous motor mode and 2) magnet-excited asynchronous generator mode. Therefore, the effect of shorted rotor windings has to be considered, if one wants to examine the process of run up to the synchronization. However, the model equations in 4.6 do not describe the asynchronous behavior of the PMSM motor drive. Therefore, the motor must start from a closed-loop speed control system, in which the motor is fed from the selected FSTPI.

4.2 SIMULINK model for PMSM motor drive

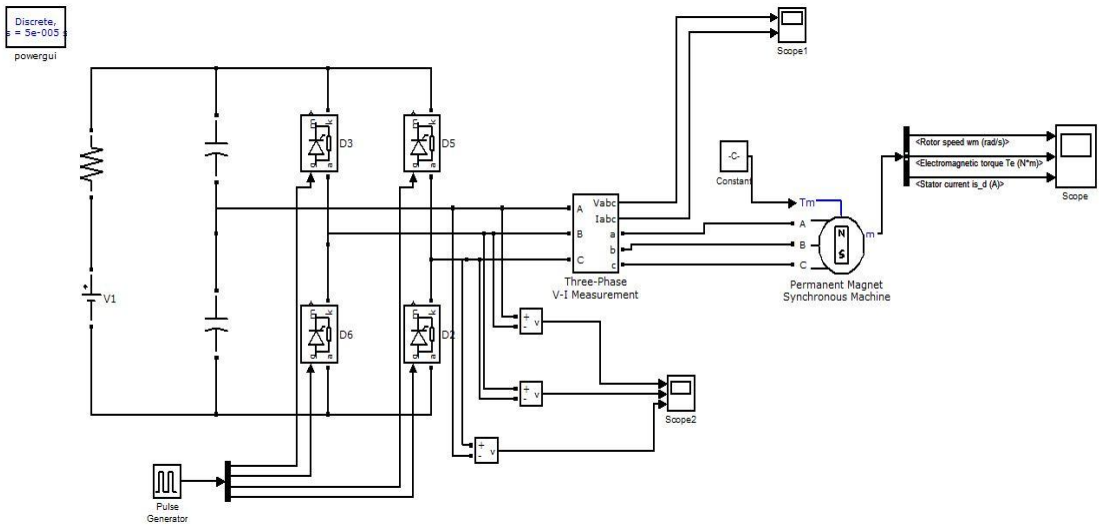

Fig. 4.5 SIMULINK model for PMSM drive

The given model was created using MATLAB - SIMULINK. The thyristors which act like switches were fired using a pulse generator. In this FSTPI, two of the output PMSM motor phases are maintained from the two inverter legs, while the third phase of the PMSM motor is fed from the dc-link at the middle point of a split-capacitor bank as shown in fig 4.5. It was not possible to obtain the results from this simulation, but best efforts will put towards its proper working. If this FSTPI fed PMSM motor model is implemented, not only there will be reduction in cost but also increase in its reliability due to the reduction in the number of switches, reduced conduction and switching losses.

CHAPTER 5

CONCLUSION

The FSTP inverter fed PMSM motor drives are found acceptable considering their cost reduction and other advantageous features. In this work, dynamic model of four-switch three-phase (FSTP) inverter fed PMSM motor system is introduced. The methods like field oriented control (FOC), direct torque control (DTC), and model predictive control (MPC) for the control of PMSM motors with FSTP inverters are discussed. A FSTP SEPIC - based inverter is discussed. This inverter improves the use of the DC bus by a factor of two compared to the conventional FSTP voltage source inverters (VSIs). Also it can produce three-phase pure sinusoidal output voltage waveforms without using the filters. A sliding mode control (SMC) [2] with fixed switching frequency was designed for the SEPIC based inverter with two different sliding surfaces called integral sliding-mode and double integral sliding-mode (DISMC). A speed controller has been designed for closed loop operation of the PMSM motor drives system so that the motor runs at the reference speed. Fairly sinusoidal output voltage and current waveforms (with only high frequency switching harmonics) are obtained for unity power factor (resistive) load.

The FSTP inverter selected from [2] is selected to control the PMSM motor in MATLAB-SIMULINK environment for investigation. The PMSM motor models suitable to be fed from the selected SEPIC based FSTP inverter are developed. However, the simulation results could not be observed.

Scope for Future Work

The selected SEPIC-based FSTP inverter is a promising candidate for the control of different AC motors. It is a suitable candidate in the control of PMSM motors for robust, reliable and smooth operation.

REFERENCES

[1] H. W. V. D. Broeck and J.D.V. Wyk, "A comparative investigation of a three-phase induction machine drive with a component minimized voltage-fed inverter under different control options," IEEE Trans. Ind. Appl., vol. IA-20, no. 2, pp. 309–320, Mar. 1984.

[2] M. S. Diab, A. Elserougi, A. M. Massoud, A. S. A. Khalik, and S. Ahmed, "A four-switch three-phase SEPIC-based inverter," IEEE Trans. Power Electron., vol. 30, no. 9, pp. 4891-4905, Sep. 2015

[3] Akin B. & Bhardwaj M. (2013). Sensored Field Oriented Control of 3-Phase Permanent Magnet Synchronous Motors C2000 Systems and Applications Team, TexasInstruments.Retrievedfromhttp://www.ti.com/general/docs/litabsmultiplefile list.tsp?literatureNumber=sprabq2

[4] C. K. Lin, J. t. Yu, L. C. Fu, T. H. Liu, and C. F. Hsiao, "Model-free predictive current controller for four-switch three-phase inverter-fed interior permanent magnet synchronous motor drive systems," IEEE/ASME AIM, Jul. 2012, pp. 1048-1053.

[5] D. Sun, J. Meng, "A single neuron PID controller based PMSM DTC drive system fed by fault tolerant 4-switch 3-phase inverter," in Proc. IEEE CIEA, May 2006, pp. 1-5.

[6] H. H. Lee, P. Q. Dzung, L. D. Khoa, L. M. Phuong, and H. T. Thanh, "The adaptive space vector PWM for four switch three phase inverter fed induction motor with DC–link voltage imbalance," IEEE Region 10 Conf., TENCON, Nov. 2008, pp. 1-6.

[7] Luukko, J. (2000). Direct Torque Control of Permanent Magnet Synchronous Machines-Analysis and Implementation. Dissertation Lappeenranta University of Technology, Stockholm.

[8] L. Wang, Y. Gao, ,A Novel Strategy of Direct Torque Control for PMSM drive Reducing Ripple in Torque and Flux", Electric Machines and Drives Conference 2007, IEMDC'07, IEEE International, Vo1.1, No.5, pp.403-406, 3-5 May 2007.

[9] Aguirre, M., Calleja, C., Lopez-de-Heredia, A., Aranburu, A., & Nieva, T., (2011) FOC and DTC comparison in PMSM for railway traction application Power Electronics and Applications (EPE 2011), Proceedings of the 2011-14th European Conference. PP-1-10.

[10] T. Ahmed, A. Das, and K. K. Halder, "Comparison of DTC and FOC for FSTPI inverter fed IPMSM drives," IEEE EICT, Feb. 2014, pp. 1-5.

[11] B. Wang, Y. He, and Y. B. Ivonne, "Four switch three phase inverter fed PMSM DTC system with non-linear perpendicular flux observer and sliding mode control," IEEE ICEMS, Oct. 2008, pp. 3206–3211

[12] C. Zhu, Z. Zeng, and R. Zhao, " Comprehensive analysis and reduction of torque ripples in three-phase four-switch inverter-fed PMSM drives using space vector pulse-width modulation," IEEE Trans. Power Electron., vol. 32, no. 7, pp. 5411-5424, Jul. 2017.

[13] Z. Zeng, C. Zhu, X. Jin, W. Shi, and R. Zhao, "Hybrid space vector modulation strategy for torque ripple Minimization in three-phase four-switch inverter-fed PMSM drives," IEEE Trans. Ind. Electron., vol. 64, no. 3, pp. 2122–2134, Mar. 2017.

[14] S. Kouro, P. Cortes, R. Vargas, U. Ammann, and J. Rodriguez, "Model predictive control A simple and powerful method to control power converters," IEEE Trans. Ind. Electron., vol. 56, no. 6, pp. 1826–1838,Jun. 2009.

[15] C. K. Lin, J. t. Yu, L. C. Fu, T. H. Liu, and C. F. Hsiao, "Model-based predictive current control for four-switch three-phase inverter-fed IPMSM with an adaptive back stepping complementary PI sliding-mode position controller," IEEE/ASME AIM, Jul. 2012, pp. 1042-1047.

[16] A.A. Hassan, J. Thomas, "Model Predictive Control of Linear Induction Motor Drive," in proc. IFAC Seoul, Korea, July 6-11, 2008.

[17] G. Beccuti, S. Mariethoz, S. Cliquennois, S.Wang, and M. Morari, "Explicit model predictive control of dc–dc switched-mode power supplies with extended Kalman filtering," IEEE Trans. Ind. Electron., vol. 56, no. 6, pp. 1864–1874, Jun. 2009.

[18] M. Cychowski, K. Szabat, and T. Orlowska-Kowalska, "Constrained model predictive control of the drive system with mechanical elasticity," IEEE Trans. Ind. Electron., vol. 56, no. 6, pp. 1963–1973, Jun. 2009.

[19] T. Geyer, G. Papafotiou, and M. Morari, "Model predictive direct torque control Part I: Concept, algorithm, and analysis," IEEE Trans. Ind. Electron., vol. 56, no. 6, pp. 1894–1905, Jun. 2009.

[20] M. B. de Correa, C. B. Jacobina, E. R. C. da Silva, and A. M. N. Lima, "A general PWM strategy for four-switch three-phase inverters," IEEE Trans. Power Electron., vol. 21, no. 6, pp. 1618–1627, Nov. 2006.

[21] Y. C. Liu, X. L. Ge, J. Zhang, and X. Y. Feng, "General SVPWM strategy for three different four-switch three-phase inverters," Electron. Lett., vol. 51, pp. 357-359, Feb. 2015.

[22] M. B. de R. Correa, C. B. Jacobina, E. R. C. da Silva, and A. M. N. Lima, "A general PWM strategy for four-switch three-phase inverters," IEEE Trans. Power Electron., vol. 21, no. 6, pp. 1618–1627, Nov. 2006.

[23] M. N. Uddin, T. S. Radwan, and M. A. Rahman, "Fuzzy-logic controller-based cost-effective four-switch three-phase inverter-fed IPM synchronous motor drive system," IEEE Trans. Ind. Appl., vol. 42, no. 1, pp. 21–30, Jan./Feb. 2006.

[24] M. N. Uddin, T. S. Radwan, and M. A. Rahman, "Performance Analysis of a Cost Effective 4-Switch, 3-Phase Inverter Fed IM Drive," Iranian Journal of Electrical and Computer Engineering, Vol. 5, No. 2, pp. 97-102, Summer-Fall 2006.

[25] Q. F. Teng, G. F. Li, J. G. Zhu,Y. G. Guo, S. Y. Li, "ADRC-based model predictive current control for PMSMs fed by three-phase four-switch inverters," IEEE IPEMC-ECCE Asia, May 2016, pp. 2724–2731.

[26] T. Q. Fang, L. G. Fei, Z. J. Guo, G. Y. Guang, and L. S-. Yuan, "ADRC-based model predictive torque control for PMSMs fed by three-phase four-switch inverters," IEEE CCC, Jul. 2016, pp. 4550-4555.

[27] S.-C. Tan, Y. M. Lai, and C. K. Tse, "Indirect sliding mode control of power converters via double integral sliding surface," IEEE Trans. Power Electron., vol. 23, no. 2, pp. 600–611, Mar. 2008.

[28] N. Li, X. Lin-Shi, A. Jaafar, E. Godoy, and P. Lefranc, “Integral sliding mode controllers for SEPIC converters,” in Proc. Control Conf., Jul. 2010, pp. 564–569.

[29] T.-S. Lee and J.-H. Liu, “Modeling and control of a three-phase fours switch PWM voltage-source rectifier in d-q synchronous frame,” IEEE Trans. Power Electron., vol. 26, no. 9, pp. 2476–2489, Sep. 2011.

[30] E. M. Fernandes, A. C. Oliveira, M. A. Vitorino, E. C. d. Santos Jr., and W. R. N. Santos, “Speed sensorless PMSM motor drive system based on four-switch three-phase converter,” IEEE IECON, Nov. 2014, pp. 902-906.

[31] J-. S. Jang, B-. G. Park, T-. S. Kim, D. M. Lee, and D-. S. Hyun, “Sensorless control of four-switch three-phase PMSM drives using extended kalman filter” IEEE IECON, Nov. 2008, pp. 1368-1372.

[32] C. K. Lin, J. t. Yu, L. C. Fu, T. H. Liu, and C. F. Hsiao, “A sensorless position control for four-switch three-phase inverter-fed interior permanent magnet synchronous motor drive systems,” IEEE/ASME AIM, Jul. 2012, pp. 1036-1041.

[33] C. Zhu, Z. Zeng, and R. Zhao, “Adaptive suppression method for DC link voltage offset in three-phase four-switch inverter-fed PMSM drives,” Electron. Lett., vol. 52, no. 17, pp. 1442 1444, Aug.18, 2016.

[34] P. Pillay and R. Krishnan, Application Characteristics of Permanent Magnet Synchronous and Brushless dc Motors for Servo Drives, IEEE Trans. on Industry Applications, v.27, p.984 996, n.5, Sept.-Oct., 1991.

[35] A Consoli and G. Scarcella and A. Testa, Industry Application of Zero-Speed Sensorless Control Techniques for PM synchronous Motors, IEEE Trans. Industry Applications, v.37, p.513-521, Mar.-Apr.,2001.

[36] S. Bolognani and M. Zordan and M. Zigliotto, Experimental fault-tolerant control of PMSM drive, IEEE Trans. Industrial Electronics, v.47, p. 1134-1141, Oct., 2000.

[37] J.-H. Jang and J.-I. Ha and M. Ohto and K. Ide and S.-K. Sul, Analysis of permanent-magnet machine for sensorless control based on high frequency signal injection, IEEE Trans. on Industry Applications, v. 39, p. 1595-2004, May-June,2003.

[38] S. Bolognani and M. Zordan and M. Zigliotto, Experimental Fault-Tolerant Control of a PMSM Drive, IEEE Trans. on Industrial Electronics, v. 47, n.5, p. 1134-1141, Oct., 2000.

[39] L. A. Ribeiro and M. C. Harke and R. D. Lorenz, Dynamic properties of back-EMF based sensorless drives, Conf. Rec. IAS Annual Meeting, 2006, v.4, p. 2026-2033, Oct., 2006.

[40] G.D. Andreescu and C. I. Pitic and F. Blaabjerg and I. Boldea, Combined Flux Observer With Signal Injection Enhancement For Wide Speed Range Sensorless Direct Torque Control of IPMSM Drives, IEEE Trans. on Energy Conversion, v. 23, p. 393-401, June, 2008.

[41] C. Caruana and G. M. Asher and M. Sumner, Performance of HF Signal Injection Techniques for Zero-Low-Frequency Vector Control of Induction Machines Under Sensorless Conditions, IEEE Trans. On Industrial Electronics, v.53 (1), p. 225-238, Feb., 2006.

[42] J. Holtz, Acquisition Of Position Error And Magnet Polarity For Sensorless Control Of Pm Synchronous Motors, IEEE Trans. on Industry Applications,v.44(4),p.1172-1180, July/Aug.,2008.

[43] E. M. Fernandes and A. C. Oliveira and A. M. N. Lima and C. B. Jacobina and W. R. N. Santos and R. D. Lorenz, A Metric For Evaluation Of The Performance Of Saliency-Tracking Self-Sensing Control Of Pm Motor, In Proc. of Brazilian Power Electronics Conference – COBEP 2013, p. 801-807, Oct., 2013.

[44] C.-T. Lin and C.-W Hung and C.-W. Liu, Position Sensorless Control for Four-Switch Three-Phase Brushless DC Motor Drives, IEEE Trans. on Power Electronics, v. 23, n.1, p. 438-444, Jan., 2008.

[45] S. Saravanasundaram and K. Thanushkodi, "Compound Active Clamping Boost Converter-Three Phase Four Switch Inverter Fed Induction Motor," International Journal of Computer Science and Network Security, Vol. 8, No. 8, pp. 358-361, August 2008.

[46] Phan Quoc Dzung, Le Minh Phuong, Tran Cong Binh, and Nguyen Minh Hoang, "A Complete Implementation of Vector Control for a Four-Switch Three-Phase

Inverter Fed IM Drive," International Symposium on Electrical & Electronics Engineering, 24-25 October 2007, HCM City, Vietnam.

[47] Wang, L.: Discrete model predictive control design using Laguerre functions. J. Process Control, pp. 131–142 (2004)

[48] Wang, L.: Use of exponential data weighting in model predictive control design. In: Proc 40th IEEE Conf. on Decision and Control (2001)

[49] Özçíra, S.; Bekiroglu, N.; Ayçiçek, E.: Speed control of permanent magnet synchronous motor based on direct torque control method. In: IEEE International Symposium on Power Electronics, Electrical Drives, Automation and Motion, pp. 268–272 (2008)

[50] Maciejowski, J.M.: Predictive Control with Constraints. Pearson Education, POD (2002) MATLAB Math Library User's Guide by the Math Works. Inc(2010)

[51] H. Kim and M. C. Harke and R. D. Lorenz, Sensorless Control Of Interior Permanent Magnet Machine Drives With Zero-Phase Lag Estimation, IEEE IAS Annual Meeting,v.2,p.86-91,2002.

[52] M. J. Corley and R.D. Lorenz, Rotor Position and Velocity Estimation for A Salient-Pole Permanent Magnet Synchronous Machine At Standstill And High Speeds, IEEE Trans. On Industry Applications, v.34, p.784-789, July-Aug., 1998.

[53] Z. Chen and M. Tomita and S. Ichikawa and S. Doki and S. Okuma, Sensorless Control Of Interior Permanent Magnet Synchronous Motor By Estimation Of An Extended Electromotive Force, Proc. IEEE IAS Annual Meeting, v. 34,p.1814-1819,July-Aug,2000.

[54] S. Bolognani and R. Oboe and M. Zigliotto, Sensorless Full-Digital PMSM Drive With Ekf Estimation Of Speed And Rotor Position, IEEE Trans. on Industrial Electronics, v.46,p.184-191,Feb.,1999.

[55] C. B. Jacobina and E. C. dos Santos Jr. and M. B. R. Correa and E. R. C. da Silva, AC motor drives with a standard number of switches and boost inductors, Proc. of IEEE Applied Power Electronics- APEC 2005, p.733-739, March, 2005.